AN ABSTRACT OF THE THESIS OF

Fang Yu Lee for the degree of Master of Science in Chemical Engineering presented on December 11, 2013

Title: Method Development for Characterizing the Hydrophobicity of Engineered Nanoparticles

Abstract approved: _____

Stacey L. Harper

Characterizing the hydrophobicity of nanoparticles can help us understand their fate and transport in the environment, as well as how nanoparticles may interact with biological systems. However, contact angle and partition coefficient have limitations in measuring the hydrophobicity of nanoparticles, thus promising methods to measuring the hydrophobicity of nanoparticles are needed. Hydrophobic interaction chromatography (HIC) and dye adsorption were used to test the hydrophobicity of nanoparticles in this study. HIC used hydrophobic interaction between hydrophobic ligand and nanoparticles to determine hydrophobicity of nanoparticles. The hydrophobicity of carboxylated nanocrystalline cellulose (CNC) is pH dependent and was used to assess the sensitivity of HIC assay. Relative hydrophobicity of metal oxides can be related to their isoelectric point (IEP) was supported by HIC. Besides, the surface coatings dominated the hydrophobicity of nanoparticles was also discussed. Dye adsorption studies were conducted using gold nanorods. By amount of hydrophobic dye adsorbed on to nanoparticles can determine their hydrophobicity. Comparing these two methods, dye adsorption can show the continuum from the hydrophobic to hydrophilic and quantified the hydrophobicity, thus it is a more promising way to measure the nanoparticle hydrophobicity than HIC.

Method Development for Characterizing the Hydrophobicity of Engineered
Nanoparticles

by
Fang Yu Lee

A THESIS

submitted to

Oregon State University

in partial fulfillment of
the requirements for the
degree of

Master of Science

Presented December 11, 2013
Commencement June, 2014

Master of Science thesis of Fang Yu Lee presented on December 11, 2013.

APPROVED:

_____

Major Professor, representing Chemical Engineering

_____

Head of the School of Chemical, Biological and Environmental Engineering

_____

Dean of the Graduate School

I understand that my thesis will become part of the permanent collection of Oregon State University libraries. My signature below authorizes release of my thesis to any reader upon request.

_____

Fang Yu Lee, Author

ACKNOWLEDGEMENTS

I would like to thank my advisor, Dr. Stacey L. Harper, for giving me great a opportunity to join this multidisciplinary team, and let me explore the field of nanotoxicology. I would also like to thank my committee members, Dr. Chih-hung Chang, Dr. Adam Higgins and Dr. Oksana Ostroverkhova for accepting my invitation to serve on my committee. I certainly thank the whole research team, especially Aaron Anderson and Zheng Zhou for supporting me during my research in the Harper laboratory. Many thanks to Bryan Harper and Josie Bonventre who helped me to revise my thesis to make it a better product.

Last but not least, I really appreciate my family and my friends who always cheered me up when I felt a bit down.

TABLE OF CONTENTS

LIST OF FIGURES

LIST OF FIGURES (continued)

LIST OF FIGURES (continued)

LIST OF FIGURES (continued)

Chapter 1: Introduction

1.1 The Application of Nanotechnology and Concern in Toxicology

The reactivity and surface area of nano-sized materials are vastly greater than larger particles due to their small size (1-100 nm in diameter). The concept of nanotechnology was first proposed in 1959 by Richard Feynman to describe the possibility of synthesis via direct manipulation of atoms. "Nano-technology" was first used as a term by the Japanese scientist Norio Taniguchi in a 1974 conference to describe the semiconductor process. By mid 90's, nanotechnology was broadly applied in engineering, pharmaceutical medicine, and commercial products. Correspondingly, the exposure of biological environment to nanomaterials began to increase while our understanding about how nanomaterials are transported and transformed through the environment has remained limited. Nanotoxicology was formalized as a field of study in 2004 and focuses on the physicochemical properties of nanoparticles to transport and how they are transformed by biologic systems to induce potential risks to human health and environment (Maynard, Warheit et al. 2011).

The need to understand which physicochemical properties of nanomaterials drive their biological interactions has become more urgent as more and more sophisticated engineering nanomaterials being developed over time. Through understanding possible pathways (ingestion, skin and inhalation) that nanoparticles travel through, we can predict the toxicity of nanomaterials and know how they affect the organism and to design safer nanomaterials. For example, the application of lipid-based nanocarriers in drug delivery systems can be used to efficiently reach target organs, accumulate in target sites and reduce the quantity of required dosage. Thus, limiting the amount of accumulation and distribution to non-specific organs (Lim, Banerjee et al. 2012). The current limits in our knowledge about nanomaterial properties and correlated behaviors limit our ability to specifically design nanomaterials to achieve a desired activity or effect.

Several physiochemical properties that can affect the toxicity of nanomaterials are: hydrodynamic size (Shvedova, Kisin et al. 2005; De Jong, Hagens et al. 2008; Jiang,

Oberdörster et al. 2009), particles shape (Chithrani, Ghazani et al. 2006; Geng, Dalhaimer et al. 2007; Pal, Tak et al. 2007; Alemdaroglu, Alemdaroglu et al. 2008; Wang, Lu et al. 2008; Perry, Herlihy et al. 2011; Zhao, Ng et al. 2013), surface chemistry or surface charge (Greenwood and Kendall 1999; Goodman, McCusker et al. 2004; Jiang, Oberdörster et al. 2009; Arvizo, Miranda et al. 2010; Qiu, Liu et al. 2010; Perry, Herlihy et al. 2011; Hanaor, Michelazzi et al. 2012), aggregation state (Takahashi, Niidome et al. 2006) and hydrophobicity (Gref, Minamitake et al. 1994; Meng, Xue et al. 2011; Xiao and Wiesner 2012). Any and all of these physicochemical properties can have a profound effect on transport, fate, uptake and ultimately, toxicity of nanoparticles due to changes in exposure and biodistribution.

1.2 The Importance of Hydrophobicity for Nanoparticle - Biological Interactions
Measuring the hydrophobicity of nanoparticles can inform us of their ability to cross cell membranes by endocytosis, or by other mechanisms include pinocytosis through the pore to penetrate the membrane and their capacity to cause bioaccumulation, then can predict their toxic potential (Kettiger, Schipanski et al. 2013). When nanoparticles come into contact with proteins or biomolecules, they form a dynamic nanoparticle protein corona whose composition can change over time by continuous association and dissociation with molecules and macromolecules in the environment. Hydrophobicity, surface chemistry, and composition of nanoparticles can influence the constituents of the protein corona. The formation of a protein corona significantly alters the surface chemical properties of nanoparticles and may influence the biocompatibility of engineered nanomaterials (Zhu, Nie et al. 2013).

Adhesion of nanoparticles to cell surface is critical when considering their toxic potential or biodegradation as their fate. Nanoparticles with higher hydrophobicity on particle surface typically show higher adhesion to bacteria cells due to large hydrophobic interaction between nanoparticles and cells (Hwang, Ahn et al. 2012). Cellular uptake mechanism of nanoparticles has been shown related to their hydrophobicity. Researchers used hydrophobically-modified chitosan (N-palmitoyl chitosan, NPCS) to show that with

an increase of degree of substitution on the nanoparticle surface, the ability of nanoparticles to interact with the cell membranes was increased and a great extent of cellular uptake was observed. The caveolae-mediated endocytosis dominated the uptake of nanoparticles with degree of substitution increased. Caveolae, a special type of lipid-raft, are flask-shaped invaginations of the plasma membrane and rich in proteins and lipids. Nanoparticles with a hydrophobic surface were taken up greater via endocytosis than with a hydrophilic surface (Chiu, Ho et al. 2010).

Hydrophobicity is also an important factor in controlling adsorption onto cells, absorption into cells, biodistribution, metabolism and excretion. Surface chemistry of nanoparticles and solution concentration influence both the amount of protein adsorbed and protein structure. Increasing surface hydrophobicity of nanoparticles can increase the amount of albumin protein adsorption to gold nanoparticles and the degree of conformation change which was caused by adsorption process; while, an increase in solution concentration increase amount of albumin protein adsorption, but decrease the degree of conformation change. This informed us that the hydrophobicity of nanoparticles influenced the protein adsorption and conformation of proteins (Sivaraman, Fears et al. 2009). The targeting performance of nanocarriers for cancer therapy can be improved by controlling various hydrophilic (polyethylene glycol, PEG) and hydrophobic (poly (N-isopropylacrylamide), PNIPAM) ratios on the surface of micelle. Micelle is surfactant aggregate disperse in aqueous solution and has hydrophilic head in contact with aqueous solution and hydrophobic tail in the micelle center. A single PEGylation without hydrophobic polymers is easier to be cleaned from the bloodstream and accumulated more in the liver and spleen. Compared single PEGylation micelle with mixed shell micelle (MSM), MSM with an effective hydrophobic polymer ratio can reduce accumulation of nanoparticles in the liver and spleen, prolong blood circulation and get efficient cancer therapy (Gao, Xiong et al. 2013). In drug delivery, targeting needs long circulation time and it is important to avoid being recognition and cleared by immune systems. In a study designed to look at improving the circulation of nanocarriers by determining the effects of the copolymer structure. Nanocarriers were produced by copolymers with hydrophobic

blocks of poly-ε-caprolactone (PCL) and hydrophilic blocks of polyethylene glycol (PEG) with varying molecular weights. PEG_{5k}-PCL_{3k} remained in the blood stream three times longer than PEG_{2k}-PCL_{3k}. PEG_{5k}-PCL_{3k} also circulated longer than PEG_{5k}-PCL_{7k}, and then PEG_{5k}-PCL_{9k}. The amount of nanocarriers in circulation after 4 hours was dependent on the relative size of the hydrophobic and hydrophilic block copolymer. (D'Addio, Saad et al. 2012). Surface properties of nanoparticles determined in vivo behaviors of nanomaterials and controlled cellular transport of nanoparticles and their biodistribution. Hydrophilic nanoparticles promote clearance and potentially minimizing environment impact; hydrophobic nanoparticles can penetrate into circulation system of fish, distribute into organs of fish and cause mortality of fish (Kim, Saha et al. 2013).

1.3 The Importance of Hydrophobicity for Nanoparticle Fate and Transport in the Environment

When nanoparticles are released, nanoparticles may form agglomerate or attach on dust, behave like aerosol in atmosphere and transport to long distance. Ultimately, they deposit on land or aqueous surfaces. Nanoparticles may agglomerate and precipitate or be transported with the flow depending on material properties and the conditions of aqueous environment such as pH, ionic strength and dissolved organic matter (DOM). Agglomeration tends to reduce the active surface area and interfacial energy and thus limits the nanoparticle reactivity. Well-dispersed nanoparticles will be transported widely and increase the chance to interact with and cause toxicity to aquatic organisms (Lin, Tian et al. 2010).

1.3.1 The Transport of Nanoparticles in Soil and Porous Media

Nanoparticles in nature soil systems have the potential to impact ground water. In particle filtration theory, the transport of nanoparticles in soil can be modeled by 4 kinds of transport in porous media: (a) gravitational sedimentation, (b) interception, (c) Brownian diffusion, and (d) retention for large agglomerates in small porous. For larger particles or agglomeration of pristine particles, sedimentation and interception dominate their transport. Brownian diffusion regulates the transport for nanoparticles. Nanoparticles

with high diffusivity tend to have a greater ability to come into collision with the soil grains. For large agglomerates with size up to microscale particles can be retained in the porous media (Elimelech, J. Gregory et al. 1995; Schrick, Hydutsky et al. 2004).

Physicochemical properties of nanoparticles can greatly influence their transport in porous media. The transport of nanoparticles is more complicated than micro-sized particles and tends to decrease with increasing particle size due to formation of agglomerates (Zhan, Zheng et al. 2008). Hydrophobic nanoparticles tend to agglomeration and precipitation out of the solution, while hydrophilic nanoparticles can be dispersed well and transport with liquid flow. Positively charged nanoparticles can be easily electrostatically attracted to environmental soil particles which are normally negatively charged, while negatively charged nanoparticles have electrostatic repulsion with soil particles and thus have higher mobility in soil matrix (Darlington, Neigh et al. 2009).

1.3.2 The Transport of Nanoparticles in Aqueous Environment
In order to study the transport and fate of nanoparticles in aqueous environment, the understanding of their interaction with nature organic matter (NOM) under a variety of solution chemistry, such as pH and ionic strength is need. NOM consists of fulvic acid and humic substance. Surface coating nanoparticles with NOM can reduce agglomeration by electrosteric stabilization or enhance agglomeration of nanoparticles from being bridging by larger NOM molecules (Christian, Von der Kammer et al. 2008; Hotze, Phenrat et al. 2010). Agglomeration of the TiO_2 was reduced by adsorption of Suwannee River Fulvic Acid (SRFA), due to increased steric repulsion (Domingos, Tufenkji et al. 2009). Similarly, NOM stabilized the dispersion of multiwalled carbon nanotubes (MWCTs) better than 1% SDS (sodium dodecyl sulfate) which was normally used as surfactant (Hyung, Fortner et al. 2007). The initial aggregation mechanism of fullerene in the presence of humic acid over different monovalent and divalent electrolyte concentrations has been discussed. The stability of fullerene increased in presence of humic acid at lower $CaCl_2$ concentration; however, there were significant aggregation of

the dissolved and unabsorbed humic acid macromolecules occurred through intermolecular bridging. Besides, humic acid adsorbed onto fullerene in the presence of NaCl and $MgCl_2$ increased stability of nanoparticles by steric repulsion (Chen and Elimelech 2007).

Other factors, for example, solution chemistry, such as pH and ionic strength has crucial effects on agglomeration of nanoparticles in nature system. Nanoparticles have positive charge in low pH and negative charge in high pH. When pH is close to their isoelectric point, repulsive forces decrease and agglomeration is promoted by van der Waals attraction (Hotze, Phenrat et al. 2010)

1.4 Research Overview

Traditional methods like contact angle and partition coefficient can be used to characterize the hydrophobicity of chemical compound; however, these traditional methods have major limitations for measuring the hydrophobicity of nanoparticles. When nanoparticles are dispersed in aqueous environment, they form different degree of agglomeration and dynamically disperse in aqueous solution. When using contact angle to measure the relative hydrophobicity of nanoparticles, nanoparticles may dynamically shift between angle of solid and liquid and angle of liquid and vapor, and thus lead to inaccuracy to measurement. The major limitation of partition coefficient in measuring the hydrophobicity of nanoparticles is that nanoparticles cannot dissolve in solution and thus they cannot reach a state of equilibrium between water and octanol phase. They form agglomeration and continuing shift between phases and can accumulate at interface of octanol/water. More detail about measurement to assess the hydrophobicity will be discussed in Chapter 2. The objective of this study was to address the limitations of traditional methods and develop a feasible way to rapidly characterize the relative hydrophobicity of nanoparticles. Hydrophobic interaction chromatography and dye adsorption will be discussed in this thesis.

Hydrophobic interaction chromatography (HIC) method was explored as a method to measure the relative hydrophobicity of nanoparticles in this study. HIC has been used in protein separation and purification since 1949 (Queiroz, Tomaz et al. 2001). In protein separation, higher hydrophobic proteins have a stronger hydrophobic interaction with the hydrophobic ligand structures in the stationary phase and thus retain in the column longer when using high salt concentrations as the mobile phase. The elution of proteins is completed as lowering hydrophobic interaction by decreasing salt concentration (Chapter 2, 3). So we can understand the relative hydrophobicity of proteins by the order of their elution. Due to HIC was used the hydrophobic interaction between hydrophobic regions of proteins and hydrophobic ligand and thus can be used to know the hydrophobicity of nanoparticles by the hydrophobic interaction between hydrophobic nanoparticles and hydrophobic ligand. The hydrophobicity of nanoparticles may from the functionalized ligand or nature of nanoparticles.
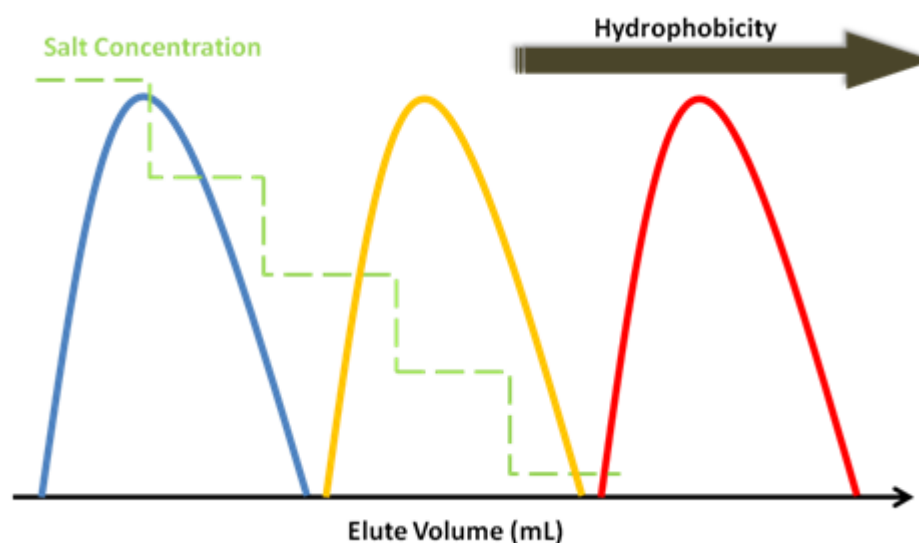
Figure 1.4.1 Theoretical chromatographs of nanoparticles on phenyl-sepharose medium

Fig 1.4.1 depicts the expected result for HIC on phenyl-sepharose medium. The blue peak represents the elution peak for the relative hydrophilic nanoparticles. When nanoparticles and hydrophobic ligands have less hydrophobic interaction, nanoparticles will elute faster. The red peak is for relative hydrophobic nanoparticles, when nanoparticles and

hydrophobic ligand have stronger hydrophobic interaction, nanoparticles have longer retention in column and elute slower. The yellow peak is for hydrophobicity of nanoparticles between blue and red peak. The green dash is the salt concentration being decreased in step.

Dye adsorption method was also explored to determine the relative hydrophobicity of nanoparticles. This adsorption method has been used in pharmaceutical studies to determine hydrophobicity of nanoparticles (Doktorovova, Shegokar et al. 2012). In this study, determining the relative hydrophobicity and hydrophilicity of nanoparticles with the use of hydrophobic Rose Bengal dye and hydrophilic Nile Blue dye, which can show continuum of nanoparticles from hydrophobic to hydrophilic.
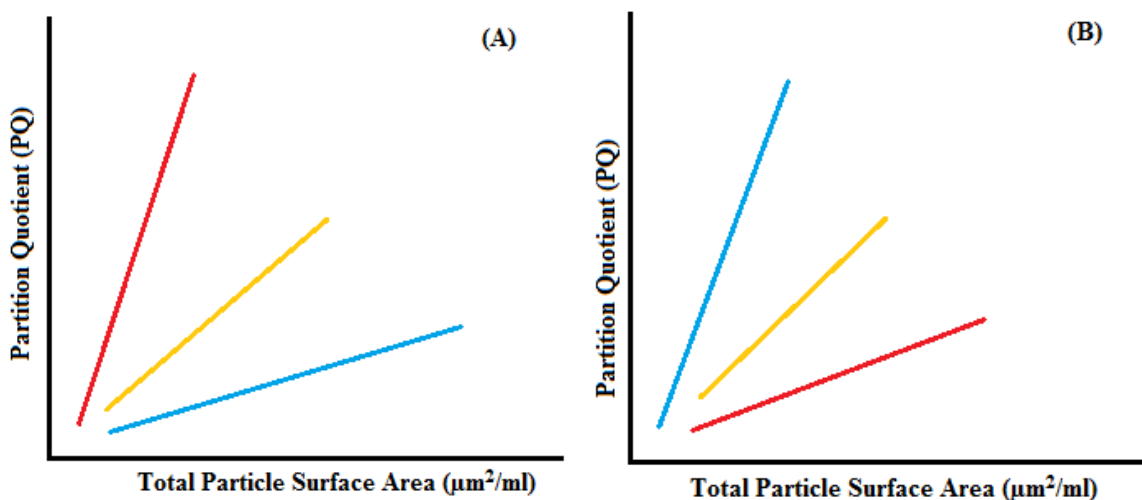
Fig 1.4.2 (A) Relative hydrophobicity qualified by adsorption of hydrophobic Rose Bengal dye onto nanoparticles (B) Relative hydrophilicity qualified by adsorption of hydrophilic Nile Blue dye onto nanoparticles

Surface hydrophobicity of nanoparticles can be qualified by the quantitative absorbance of hydrophobic Rose Bengal dye onto nanoparticles, the amount of adsorbed dye increase as total surface area increase. The partition coefficient (PQ) was calculated against surface area. In the Rose Bengal dye adsorption study, nanoparticles with higher

hydrophobicity (red line) would have increased adsorption as surface area increased; a steeper slope is indicative of higher hydrophobicity (Fig 1.4.2 (A)). Correspondingly, in the Nile Blue dye adsorption study, nanoparticles with higher hydrophilicity (blue line) would have increase adsorption as surface area increased; a steeper slope is indicative of higher hydrophilicity (Fig 1.4.2 (B)). More detail about calculating PQ value is in Chapter 2.2.4.

1.4.1 Material Selection

In order to test the feasibility of HIC, there were four hypotheses were proposed. First, surface chemistry of carboxylated nanocrystalline cellulose (CNC) is pH dependent. When CNC are dispersed in low pH environment, they are surrounded by H^+ and show hydrophobic properties; when CNC are dispersed in high pH environment, they are surrounded by OH^- and show hydrophilic properties. Second, the hydrophobicity of metal oxides can be predicted based on isoelectric point (IEP). The rationale is that if pH is smaller than the IEP of the metal oxide, more H^+ would be available on the surface of the metal oxides and makes them relative hydrophobic and possess a positive charge. Conversely, when pH is larger than the IEP, more OH^- would be available on the surface of the metal oxides, causing them to become relatively hydrophilic and have negative charge (Fig 1.4.3). Third, yttrium oxide (Y_2O_3) is more hydrophobic than silicon dioxide (SiO_2). The IEP of Y_2O_3 is 9.6 and 1.0 for SiO_2 at pH 7.4 (Fig B.1). From Fig 1.4.3, we can know Y_2O_3 is hydrophobic and SiO_2 is hydrophilic at pH 7.4. Fourth, silicon dioxide (SiO_2) is more hydrophobic than PEGylated silicon oxide (PEGylated- SiO_2). Chapter 4 would discuss more about these four hypotheses.
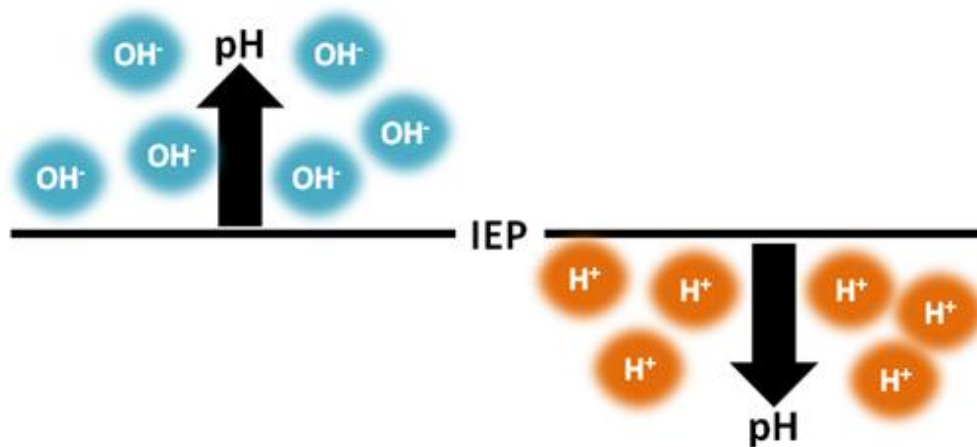
Fig 1.4.3 An illustration for the rationale of predicting the relative hydrophobicity of nanoparticles from the IEP at a given pH

Chapter 2: Literature Review

This chapter basically covers the physicochemical properties that affect exposure and hazard of nanoparticles and methods to measure the hydrophobicity

2.1 Nanomaterial Physicochemical Properties that Affect Exposure and Hazard

2.1.1 Nanomaterial Primary Particle Size

Toxicology studies have shown increased toxicity of nanomaterials compared to micro-scale materials of the same composition due to their small size and large reactive surface; they have greater ability to facilitate the cellular uptake and distribute wider than micro-sized materials. However, it is unclear if it is true for a wide range of nanoparticles to have higher toxicity. A study compared a series nanoparticle of Fe_2O_3, Fe_3O_4, TiO_2 and CuO with micrometer particles of the same composition and expose to human alveolar epithelial cell line (A549). Iron oxides showed low toxicity and no great difference with between nano and micro particles. The toxicity of TiO_2 is from their crystal structure. CuO nanoparticles showed much more toxicity than CuO micrometer particles (Karlsson, Gustafsson et al. 2009). Comparing the toxicity of micro- and nano-sized silver nanoparticles in human hepatocyte cell line L02, nano-sized silver nanoparticles cause cell morphology displaying shrinkage and showing irregular shape (Liu, Guan et al. 2011). Nanoparticles hydrodynamic size can change with different pH. When pH of nanoparticles near their isoelectric point, which means zero charge on their surface, the electrostatic repulsion force is weakened and van der Waals can overcome repulsive forces and attraction is stronger, and thus increase the hydrodynamic size (Jiang, Oberdörster et al. 2009). Biodistribution of nanoparticles is also affected by their size. Injection of 10nm, 50nm, 100nm and 250nm gold nanoparticles (Au-NPs) into rats, exposed for 24 hours found that the 10nm Au-NPs were spread the widest and the larger size nanoparticles were only found in the blood, liver and spleen (De Jong, Hagens et al. 2008).

2.1.2 Agglomeration State of Nanomaterials

When nanoparticles are dispersed in liquids, the hydrodynamic size of nanoparticles is usually larger than primary size as they form different degrees of agglomeration. Agglomeration is a process of nanoparticle gathering into a mass when they are dispersed in aqueous environment. To what extent of the agglomeration state will influence fate, transport, cellular uptake and reactivity of nanoparticles is largely unknown.

Agglomeration states of nanoparticles induce great influence in their transport, uptake and interaction with biologic systems. After dispersing nanoparticles in solution, nanoparticles may form agglomeration or aggregation or remain singlet. The difference between agglomeration and aggregation is that for agglomeration, nanoparticles are attached to each other by weak van der Waals; for aggregation, nanoparticles are held by strong chemical bond (Jiang, Oberdörster et al. 2009). Agglomeration can alter nanoparticle distribution, and thus affect the fate and toxicity of nanoparticles in biologic systems. When cerium oxides being dispersed in culture medium, compared with larger size (250-500nm), small size (25-50nm) nanoparticles formed agglomeration rapidly (Limbach, Li et al. 2005). A study investigated that how the agglomeration state affected cytotoxicity carbon nanotube (CNT) with human MSTO-211H cells and showed that, in contrast to nanoparticles, the agglomerated CNT showed more adverse effects than well-disperse CNT (Wick, Manser et al. 2007). Conversely, the exposure of gold particles of 50 and 250nm to lung and how their agglomeration states influenced biologic response was discussed. The result showed that single gold nanoparticles did not pose greater toxicity than their agglomerates in pulmonary inflammation (Gosens, Post et al. 2010). A study has investigated the role of the agglomeration state in rat pulmonary response by exposing 5, 10-30, 50nm TiO_2 aerosols to Fisher 344 male rats at same concentration and inhaled for 6 hours. The agglomeration state for aerosols is composed of small agglomerates (<100nm) and large agglomerates (>100nm). Significant oxidative stress was observed in all small agglomeration; however, there is no oxidative stress effects for larger agglomerates (Noel, Charbonneau et al. 2013).

2.1.3 Nanomaterial Shape

Recently studies have shown that nanoparticle shape can have profound effects on the cellular uptake, internalization rate, and circulation of nanoparticles. Cytotoxicity of hydroxyapatite (nHA) nanoparticles is shape (different specific surface area) and cell specific. Needle and plate shaped-nHA were found to be more toxic to BEAS-2B cells compared with round nHA in a recent study by Zhao and colleagues. However, these three shapes of nHA did not cause significant death in RAW264.7 cells (Zhao, Ng et al. 2013). In another study, nanoparticle uptake was found to be dependent on the shape of gold nanoparticles with the uptake of gold nanorods is 375% less than spherical gold nanoparticles into mammalian cells. Moreover, the uptake was greater for rod-shaped gold nanoparticles with low aspect ratio (1:3) than higher aspect ratio (1:5)(Chithrani, Ghazani et al. 2006). Cylindrical PEG hydrogel particles had higher internalization rates than cubic particles and particles with high aspect ratio the internalization rate is four times faster than low aspect ratio nanoparticles by HeLa cell (Perry, Herlihy et al. 2011). Highly stable, polymer assemblies called filomicelles with similar surface chemistry as spherical micelle have shown that the circulation of filomicelles in rodent is ten times longer than sphere one. Under fluid flow, spheres and shorter filomicelles were more easily taken up by the cell than longer filomicelles (Geng, Dalhaimer et al. 2007). The antibacterial activity of silver nanoparticles has been shown depend on their shape. At a given concentration, truncated triangular silver nanoparticles are found to be more effective in inhibiting the growth of E.coli than spherical and rod-shaped silver nanoparticles. This can be explained by the percent of active facets {1, 1, 1} which have more high-atom-density present in nanoparticles. Truncated triangular nanoparticles contain more {1, 1, 1} facet than other two nanoparticles and thus have higher antibacterial activity (Pal, Tak et al. 2007).

To summarize, rod shape and high aspect ratio nanoparticles tend to cause higher cytotoxicity, higher internalization rate than spherical nanoparticles in vitro; however, sphere and lower aspect ratio nanoparticles are more easily taken up by the cell than rod

and higher aspect ratio. For in vivo study, rod-shaped nanoparticles have longer circulation and higher uptake amount than spherical nanoparticles.

2.1.4 Zeta Potential

When nanoparticles are dispersed in a solution, ions are adsorbed onto the nanoparticles surface, ionizing the nanoparticles and establishing a net surface or zeta potential. The absolute value of zeta potential can inform us the stability of solution. When nanoparticles have high zeta potential, the repulsion exceeds attraction and confers dispersion stability and then can resist agglomeration; when nanoparticles have low zeta potential, the attraction exceeds repulsion and form agglomeration (Greenwood and Kendall 1999; Hanaor, Michelazzi et al. 2012).

The relation between zeta potential, pH and isoelectric point has been discussed. Zeta potential can be adjusted by changing solution pH. Using a small amount of carboxylic acid as additive can impart a negative charge nanoparticles and cause their zeta potential to drop (Hanaor, Michelazzi et al. 2012). When pH is far from isoelectric point of nanoparticles, the absolute value of zeta potential is higher; when pH approach isoelectric point of nanoparticles, the absolute value of zeta potential is low. If pH is higher than the isoelectric point of nanoparticles, there is more OH^- on the surface of nanoparticles and make nanoparticles have negative charge. If pH is lower than the isoelectric point of nanoparticles, nanoparticles are surrounded by more H^+ and have positive charge (Jiang, Oberdörster et al. 2009).

Zeta potential can largely influence cellular uptake through the electrostatic interaction. Most cell surfaces possess a negative charge, thus nanoparticles with positive zeta potential can be internalized faster than nanoparticles with a negative and neutral zeta potential. Gold nanoparticles with positive charge (Au^+) showed more uptake in plasma membrane, rather than negative (Au^-), neutral (Au^0) and zwitterionic ($Au^{+/-}$) gold nanoparticles. Furthermore, positive AuNP showed more membrane potential change than negative (Au^-), neutral (Au^0) and zwitterionic ($Au^{+/-}$). Positive charges on AuNPs

have also been shown to perturb the cell membrane and increase cytotoxicity in human bronchial epithelial cells (BEC cells) (Arvizo, Miranda et al. 2010). The internalization rate of nanoparticles also is affected by their zeta potential. 84% positively charged PEG hydrogel nanoparticles were internalization by HeLa cell; however, those with a negative charge showed no significant amount change in internalization (Perry, Herlihy et al. 2011). Cationic nanoparticle clusters caused eight times more lysis than the anionic one by strong electrostatic interaction with negative charge lipid layer (Goodman, McCusker et al. 2004).

In summary, the surface charge of nanoparticles affects the uptake of nanoparticles, positive nanoparticles internalized faster by cell than particles with negative or neutral charge.

2.1.5 Nanomaterial Surface Chemistry

Many studies have shown that the influence of surface chemistry is greater than the influence of core and plays a significant role in controlling their cytotoxicity, circulation, accumulation, dispersion and cellular uptake. Nanoparticles can be designed with specific surface functional groups for applications in biomedicine, semiconductors, solar energy, drug delivery and therapeutics to cure diseases. Multifunctional nanoparticles can be prepared by a series of organic reactions including surface silanization, amine-azide conversion, azide-alkyne 'click' chemistry, thiol and amine click chemistry and amide coupling (McCarthy, Davies et al. 2012). The following are a few examples of alterations in behavior that are dependent on surface chemistry.

Modifying surface chemistry of nanocrystal quantum dots (QD) altered their cytotoxicity illustrating that the core effect could be modified through surface chemistry (Hoshino, Fujioka et al. 2004). Surface coating of engineered nanoparticles control surface chemistry of nanoparticles and may dominate the effect of the nanoparticle core. Aqua-nC_{60} showed more hydrophobicity than THF-nC_{60}. Coating Tetrahydrofuran (THF) onto fullerene lead to partial hydroxylation of fullerene surface, forming hydrogen bond with

water to make THF-nC$_{60}$ hydrophilic than Aqua-nC$_{60}$ (Xiao and Wiesner 2012). Cetyltrimethylammonium bromide (CTAB) is a surfactant which was coated onto gold nanoparticles to assist their dispersion and recently has been proved causing toxicity. A study showed that spherical gold nanoparticles are not inherently toxic to human skin cells; however, gold nanoparticles showed high toxicity in the presence of CTAB (Wang, Lu et al. 2008; Qiu, Liu et al. 2010). Modification of gold nanoparticles to phosphatidylcholine (PC) instead of CTAB surface chemistry reduced agglomeration and cytotoxicity of gold nanoparticles (Takahashi, Niidome et al. 2006).

Polyethylene glycol (PEG) is a biodegradable ligand applied to nanoparticles to improve their function as drug delivery systems. PEGylation of nanoparticles improves the blood circulation time and decreases liver accumulation in mice (Gref, Minamitake et al. 1994). Mesoporous silica nanoparticles (MSNP) with a polyethyleneimine-polyethylene glycol copolymer (PEI-PEG copolymer) can disperse better by steric hindrance and electrostatic repulsion and reduce opsonization, and enhance targeted delivery to specific cell populations (Meng, Xue et al. 2011). The cellular toxicity of cationic nanoparticles is due to tight surface membrane binding and thus facilitates particles wrapping and cellular uptake. Polyethyleneimine (PEI) coated mesoporous silica nanoparticles (MSNP) can facilitate cellular uptake to increase drug delivery payload and improve nucleic acids delivery for therapeutic. Nevertheless, PEI could interfere with siRNA delivery and cause toxicity. High molecular weight (25kD) PEI polymers display high cationic density, inducing toxicity and damage to negatively charged cell line stain. On the other hand, low molecular weight PEI polymers are inefficient for gene delivery but enough for delivering antitumor drug into cancer cells. Thus, it is important and necessary to select optimal polymer length to balance the efficiency of drug delivery and cytotoxicity (Xia, Kovochich et al. 2009).

2.2 Characterization of Hydrophobicity

2.2.1 Contact Angle

The contact angle is the angle that liquid/vapor interface onto the solid substrate. When contact angle is higher than 90 degree angle, droplet is hydrophobic; lower than 90 degree angle, droplet is hydrophilic (Fig2.2.1). Surface roughness and surface energy can affect the wettability of the solid surface. On a smooth surface, contact angle (θ) is given by Young's equation (Eq. (1)).

$$\cos\theta = \frac{r_{SV} - r_{SL}}{r_{LV}} \quad (1)$$
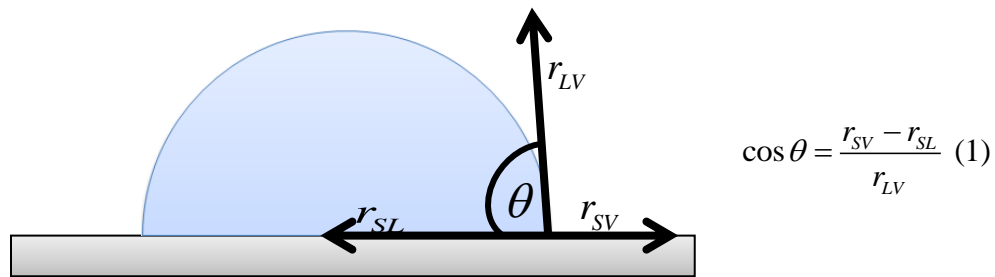
Figure 2.2.1 An illustration of contact angle

r_{SV} is the solid-vapor surface tension, r_{SL} is the solid-liquid surface tension and r_{LV} is the liquid-vapor surface tension. The contact angle on surface can be usually modeled by two theories – Cassie's theory and Wenzel's theory.
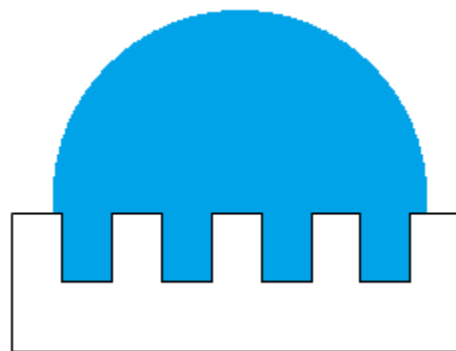
Wenzel's theory assumes the liquid fill into notch. (Wenzel 1936; Wenzel 1949)

$$\cos\theta' = r\cos\theta \quad (2)$$

θ': the apparent contact angle on surface

r: the roughness ratio is real surface area over apparent surface area

(wetted surface)

Figure 2.2.2 Wenzel's theory in contact angle (He, Patankar et al. 2003; Patankar 2003)
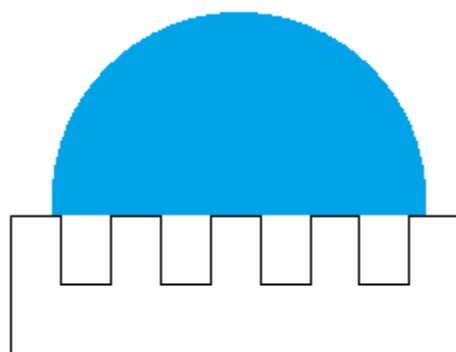
Cassie's theory assumes the liquid is lifted up and not fill into the notch.

$$\cos\theta' = \delta\cos\theta + \delta - 1 \quad (3)$$

(Cassie and Baxter 1944; Cassie 1948)

θ' : the apparent contact angle on surface

r : the roughness ratio

δ :area function of the surface

(composite surface)

Fig 2.2.3 Cassie's theory in contact angle (He, Patankar et al. 2003; Patankar 2003)

Wenzel's (Eq. (2)) and Cassie's (Eq. (3)) theories measure different contact angle on the same surface. However, previous studies did not discuss about when and which theory to use until 2003. A study proposed that there can be two different contact angles on same rough surface, depending on how the droplet is formed. The wetted surface is formed by dropping droplet from some height (Fig2.2.2); the composite surface is formed by dropping droplet gently (Fig2.2.2) (He, Patankar et al. 2003; Patankar 2003). The sessile drop method is used to measure the contact angle through the goniometers and using an optical system to capture the profile of the pure liquid on the solid substrate. Thus, Wenzel's theory that the wetted surface is formed by dropping droplet from some height would be better to describe the sessile drop method.

Contact angle has been used widely to measure the hydrophobicity of materials; however, the problems were arised when using this method to measure the hydrophobicity of nanoparticles. Due to dynamic nature of nanoparticles, the nanoparticles may continuously shift and form agglomeration between the angle of liquid and solid and the angle of liquid and gas and thus cause uncertainty for measurement. Besides, the high surface area of nanoparticles may cause reaction between nanoparticles and solid substrate which may not happen for microsized particles.

2.2.2 Partition Coefficient (log P or log K_{ow})

$$logP = log\left(\frac{Solute\ in\ non-polar\ solvent}{Solute\ in\ polar\ solvent}\right) \quad (4) \quad or \quad logKow = log\left(\frac{Solute\ in\ octanol}{Solute\ in\ water}\right) \quad (5)$$

The 1-octanol/water partition coefficient is a widely used method to determine the hydrophobic property of chemicals. Partition coefficient is the concentration ratio of a chemical compound in octanol (non-polar solvent) and in water (polar solvent) at equilibrium. Octanol and water are premixed and equilibrated for 24 hours before measuring, mixing materials with octanol-water, shaking mixture for 24 hours on a shaker and standing for 3 hours. A hydrophobic chemical with high partition coefficient are preferentially distributed to the hydrophobic phase (Xiao and Wiesner 2012).

However, there are some limitations to using the partition coefficient to measure the hydrophobicity of nanoparticles. First, partition coefficient is only accurate for uncharged materials. Second, it is not suitable for materials when their hydrophobic properties changes with pH. For nanoparticles, the size, surface charge and hydrophobicity can change with pH. Third, nanoparticles are not in solution, thus, they do not go into a state of equilibrium between water and octanol phase. They are dynamic and can reversibly form agglomerations which can shift their distribution between phases and form aggregation and accumulate at interface of octanol/water (Xiao and Wiesner 2012).

2.2.3 Hydrophobic Interaction Chromatography (HIC)

Hydrophobic Interaction Chromatography (HIC) has been used in protein separation and purification for a long time, and today has become a powerful method at the laboratory scale and in industry. It was first used in 1949 by Shepard and Tiseliusin who described the method as "salting-out" (Cronin 2006). In 1973, the term "hydrophobic interaction chromatography" (HIC) was first used by Hjertén (Hjerten 1973). By using salt to promote hydrophobic adsorption, Porath proposed alternative name and described it as – "salt-promoted adsorption chromatography" (Queiroz, Tomaz et al. 2001). HIC was only

applied in separation of proteins, the related literature about applying HIC in measuring the hydrophobicity of nanoparticles has not yet been proposed.

HIC is conducted by running a high ionic strength salt buffer through a chromatography column lined with hydrophobic ligands (Fig 2.2.4). Proteins will precipitate and bound to the hydrophobic ligands, and thus also called "salt-out" effect. Proteins are eluted by decreasing the ionic strength in a linear or an in-step manner (Queiroz, Tomaz et al. 2001). There are several factors that can affect the optimization and performance of HIC for protein
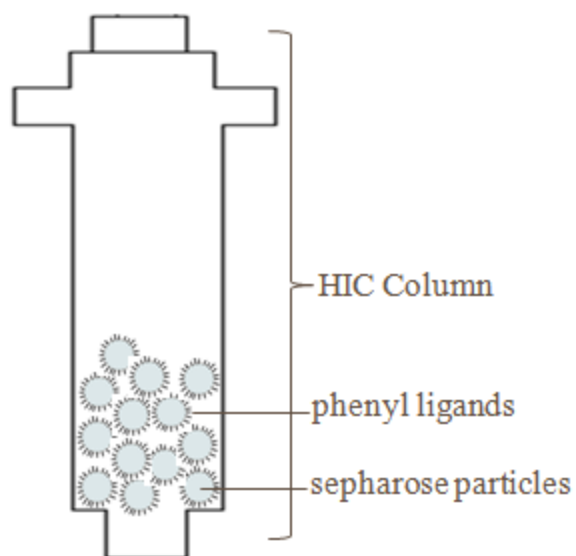
Fig 2.2.4 Phenyl ligands on separose particles

separation that would need to also be considered for measuring the hydrophobicity of nanoparticles. In stationary phase, factors such as hydrophobic ligand, ligand substitute density and ligand chain length should be considered. In mobile phase, salt types, concentration of the salt, pH, temperature, elution rate are also important for HIC performance (Mahn and Asenjo 2005).

Stationary Phase:

A. The Option of Ligand on the Medium

The most common use ligands used in HIC are linear chain alkanes (like butyl, octyl) and aromatic groups (phenyl). The strength of hydrophobic interaction increases as the alkane chain length increases; however, the selectivity of adsorption or resolution may decrease due to the increasing adsorption effect. Moderately strong ligand binding is important, since extremely strong binding may cause irreversible reactions, like denaturation in the case of proteins. Therefore, moderately hydrophobic ligand binding is more practical and allow for elution by simply reducing ionic strength

(Hofstee 1975). For nanoparticles, strong binding would not cause denaturation but may lead to strong hydrophobic interaction between nanoparticles and ligands and decrease the resolution.

B. The Degree of Substitution for Hydrophobic Ligand

The degree of substitution is a critical parameter in the adsorption of proteins. For example, increasing the degree of sepharose substitution increases the probability of forming multipoint attachment and thus increases the binding capacity of stationary phase (Ochoa 1978; Lienqueo, Mahn et al. 2007). Another study showed that the capacity of agarose gel increase with increasing the degree of substitution; however, if the degree of substitution is extremely high, it would difficult to complete desorption process (Rosengren et al. 1975). Similarly, it will be hard to achieve desorption for nanoparticles if the degree of substitution is too high.

Mobile Phase:

A. The Influence of pH on HIC

High pH weakens the hydrophobic interaction between proteins and the hydrophobic ligands, due to a change in the proteins charge and hydrophobicity. Low pH strengthens the hydrophobic interaction and increase the retention of proteins (Hjerten 1973; Hjertén, Rosengren et al. 1974). When pH of mobile phase is close to isoelectric point of proteins, the net charge of proteins is equal to zero. When the electrostatic repulsion between the proteins and ligand reaches a minimum hydrophobic interactions are maximized (Lienqueo, Mahn et al. 2007). The control of pH value is one of the dominant factors in determining the proteins retention in the column. This principle could readily be applied to assess the hydrophobicity of nanoparticles. Metal oxide nanoparticles are sensitive to pH, due to the isoelectric points of metal oxides are measured at a given pH and thus affect the hydrophobicity of metal oxides which was discussed in Chapter 1.4.

B. The Influence of Temperature on HIC

Raising the temperature enhances hydrophobic bonding while lowering the temperature reduces the hydrophobic interaction (Hjerten 1973; Hjertén, Rosengren et al. 1974). When temperature is increased, the stability of nanoparticles is increased by hydrogen bond and van der waals interaction and thus enhance the hydrophobic interaction (Ochoa 1978). Entropy is always positive and free energy is negative during this spontaneous process. Thus, the higher the temperature, the larger the free energy and the longer the retention time in the column (Queiroz, Tomaz et al. 2001). As increasing temperature for nanoparticle case, their Brownian motion would be increased and thus enhance their hydrophobic interaction. However, temperature is not a major factor to control the elution and thus should be held constant when running the HIC.

C. The Influence of Salt Selection

The desired precipitation and separation of proteins can be enhanced with the follow of Hofmeister series (Porath 1987). The ion which is more close to the left-hand side of the series (such as NH_4^+, PO_4^{3-} etc) can promote hydrophobic interactions and increase surface tension which increases the retention time and protein separation (Fig 2.2.4). However, as ions move to the right-hand side of the series (such as SCN^-, $Ba2^+$ etc) (Fig 2.2.4), the strength of hydrophobic interaction is decreased (Xia, Nagrath et al. 2004). Similarly, the retention of nanoparticles can follow the Hofmeister series which was used in protein separation.

Increasing salting-out effect

$\longleftarrow$

Anions: PO_4^{3-}, SO_4^{2-}, CH_3COO^-, Cl^-, Br^-, NO_3^-, ClO_4^-, I^-, SCN^-

Cations: NH_4^+, Rb^+, K^+, Na^+, Li^+, Mg^{2+}, Ca^{2+}, Ba^{2+}

$\longrightarrow$

Increasing salting-in effect
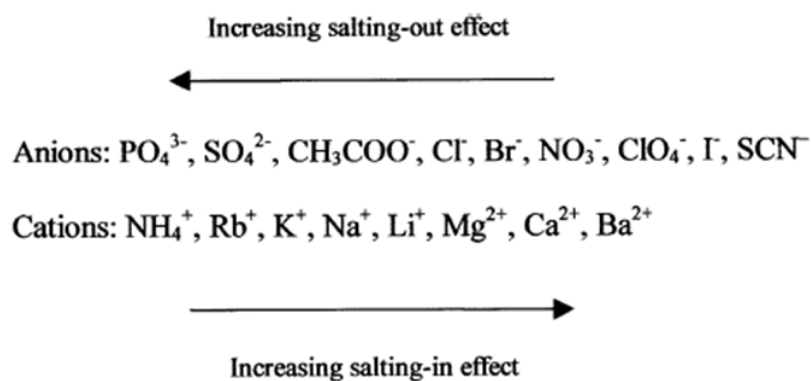
Fig 2.2.5 Illustration of the Hofmeister series (Porath 1987)

D. The Influence of Salt Concentration on HIC

The concentration of salt used during HIC strongly influences not only the selectivity of proteins adsorbed but also the strength of hydrophobic interaction between the ligand and the proteins (Oscarsson and Kårsnäs 1998). A moderately high salt concentration can increase ionic strength and surface tension, promoting the interaction between the proteins and the ligand attached onto the medium. The increase in retention time improves protein separation. However, overly high salt concentration may cause proteins denaturation (Queiroz, Tomaz et al. 2001). For nanoparticles, the consideration for salt concentration is also important. Critical concentration for nanoparticles to form agglomeration is around 100mM (Jiang, Oberdörster et al. 2009)

2.2.4 Dye Adsorption Method

Rose Bengal partition method was developed to determine the hydrophobicity of uncoated nanoparticles by Muller in 1986. The dye adsorption method uses Rose Bengal (RB) (Fig 2.2.5), a xanthene dye, to measure surface hydrophobicity of nanoparticles. Rose Bengal is hydrophobic because of the chloride ions (Cl$^-$) in Rose Bengal structure. Surface hydrophobicity is qualified by adsorption
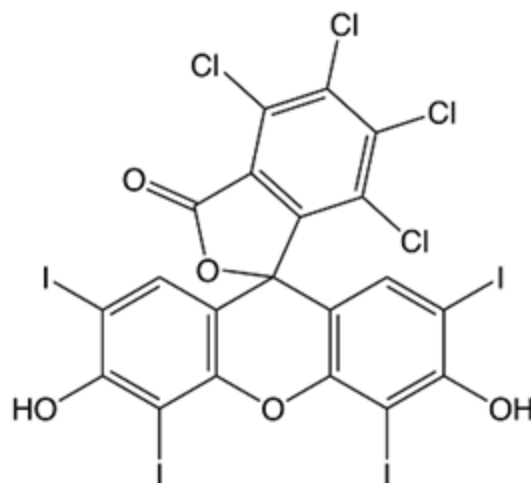
Fig 2.2.6 Chemical structure of Rose Bengal

of hydrophobic Rose Bengal dye onto nanoparticles based on their surface area. Rose Bengal is either adsorbs to the nanoparticles surface or remains in the aqueous phase depending on the hydrophobicity of the nanoparticle surface. Nanoparticles are removed from the solution along with any Rose Bengal that was bound to it. The remaining Rose Bengal which was not bound to nanoparticles can be easily measured by

spectrophotometry. Rose Bengal adsorbed onto the surface of nanoparticles shows more hydrophobic property than less adsorbed one (Rainer H. Müller 1997).

This method assumes dye is stable over incubation; the only change is the amount of dye in solution after exposing dye to the nanoparticles. The relative hydrophobicity can be determined by calculating Partition Quotient (PQ) against hydrodynamic surface area. A larger slope indicates more adsorption of Rose Bengal on nanoparticles and hydrophobicity (Xiao and Wiesner 2012).

$$[\text{Mass of adsorbed dye}] = [\text{Mass of original dye}] - [\text{Mass of unadsorbed dye}] \quad (6)$$

$$PQ = \frac{\text{Mass of RB adsorbed onto particle surface}}{\text{Mass of unadsorbed RB}} \quad (7)$$

Hydrophilic Nile Blue dye is used to assess the hydrophilicity of nanoparticles based on the same procedures and PQ calculations as for Rose Bengal. The hydrophilicity of Nile Blue is from amino group (NH_2^+) onto its structure. The using of hydrophilic Nile Blue dye can show a continuum from hydrophobicity to hydrophilicity. For example, the relative hydrophobicity of two hydrophilic nanoparticles can be interpreted from adsorption of hydrophilic dye. The lager slope in PQ against total surface area (Fig 1.4.2 (B)) is indicative of less hydrophobic particles.
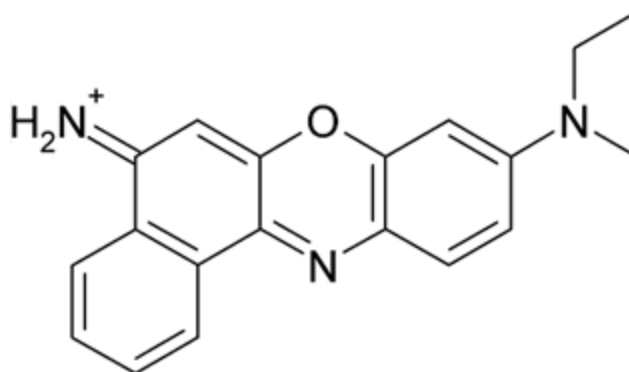
Fig 2.2.7 Chemical structure of Nile Blue

Chapter3: Experiment Design

3.1 Hydrophobic Interaction Chromatography

3.1.1 Materials

Phenyl-sepharose CL-4B (~40μmol/ml, pH4~12), SiO_2 (silicon dioxide, nanopowder, 12nm avg size, 99.8% trace metal basis), $(SiO_2)x(Al_2O_3)y$ (silicon dioxide with alumina doped 10 wt% dispersed in water, x=0.9-0.95, y=0.05-0.1, 99.99% trace metal basis, <50nm) and Y_2O_3 (yttrium (III) oxide, nanopowder, <50nm) purchased from Sigma Aldrich (St. Louis, MO). Carboxylated nanocrystalline cellulose (CNC, 5.5% dispersion) was bought from Bio Vision Technology Inc. $(NH_4)_2SO_4$ (ammonium sulfate, granular) and Na_2HPO_4 (sodium phosphate, dibasic, anhydrous, granular, 99.1%) were purchased from Macron Chemicals (Center Valley, PA). NaH_2PO_4 (sodium phosphate, monobasic, anhydrous, 99%) was purchased from Fisher Scientific (Fair Lawn, NJ). C_2H_5OH (ethanol, HPLC-UV reagent grade, anhydrous, 99.8%) was from Pharmco-Aaper (Shelby, KY). 2.5ml columns (10μm filter pore size) were purchased from Boca Scientific (Boca Raton, FL). NanoPure water was from Milli-Q ultra-pure system used to prepare all samples, system resistivity was 18MΩcm.

3.1.2 Stock Solution Preparation

28.392g Na_2HPO_4 and 23.996g NaH_2PO_4 were dissolved separately in 1 liter NanoPure in order to prepare 0.2M salt solution. Next, 160 ml NaH_2PO_4 solution and 840 ml Na_2HPO_4 solution were mixed together and adjusted to final pH of 7.5. pH was adjusted by 0.2M NaH_2PO_4 and Na_2HPO_4 solution to avoid other ions interfering with the elution. To make the eluent, NanoPure was used to dilute phosphate buffer to final concentrations of 50mM, 40mM, 30mM, 20mM, and 10mM.

Stock solutions of metal oxides (SiO_2, $(SiO_2)x(Al_2O_3)y$, Y_2O_3) were ultrasonicated for 20 minutes to disperse them, PEGylated-SiO2 was ultrasonicated for $45-60$ minutes so that the PEG polymer was dispersed well in ultrapure water. CNC was diluted from 5.5% to 100ppm with NanoPure and pH was adjusted to 4 by HCl and 12 by NaOH.

3.1.3 PEGylated-SiO$_2$ Nanoparticles Preparation

The PEGlyated-SiO$_2$ were synthesized according to the following procedure (Oh, Lee et al. 2009). Polyethylene glycol (PEG) 10g 1500 g/mol was added to 75mL of NanoPure water in 250ml flask and stirred until all of the PEG dissolved. The solution was cooled to 0℃ in an ice bath for 1 hour. Then 5ml vinyltrimethoxy silane was added and the solution was incubated in an ice bath for 24 hours. After 24 hours, replenishing ice bath and 100μL concentrated NH$_4$OH was added to the reaction mixture over 10 seconds while stirring. The mixture was kept at 0℃ for 2 hours and then vacuumed to obtain dry powder in a fume hood at room temperature for 72 hours.

3.1.4 Chromatography Column Preparation

Phenyl-sepharose CL-4B was stored in 4°C refrigerator. Phenyl-sepharose CL-4B slurry was slowly packed into a 2.5mL column. Ultrapure water was pumped into column to ensure the bed was compacted well to 2cm. Care was taken during packing to avoid producing void or bubble during the packing process.

3.1.5 Nanoparticle Evaluations

A. CNC

To condition the chromatography bed, 5 times of bed volume buffer A (50mM Phosphate Buffer and 2M (NH$_4$)$_2$SO$_4$), 10mL was run through the column using a syringe pump flow rate of 1mL/min to ensure the column reached equilibrium. To support the hypothesis for this study, 1mL of 100ppm CNC were injected into the column. After injecting, the flow rate was started at 1ml/min. Elute nanoparticles through the column and reduces hydrophobic interaction by decreasing the (NH$_4$)$_2$SO$_4$ salt concentrations in step manner from 2M, 1.5M, 0.5M, to 0M and collect 4mL for each salt concentration, keep running NanoPure into column until elution concentration reach zero.

B. Metal Oxides

- **Al_2O_3-SiO_2**

To condition the chromatography bed, 5 times of bed volume buffer A (50mM Phosphate Buffer and 0.1M $(NH_4)_2SO_4$), 10mL was run through the column using a syringe pump flow rate of 1mL/min to ensure the column reached equilibrium. To support the hypothesis for this study, 10μL of 100ppm Al_2O_3-SiO_2 were injected into the column. After injecting, the flow rate was started at 10ml/min. Elute nanoparticles through the column and reduces hydrophobic interaction by decreasing $(NH_4)_2SO_4$ buffer concentrations in step manner from 0.1M, 0.05M, 0.01M, to 0M, followed by 10%, 20%, 40%, 80%, and 100% ethanol as last stage to reach 100% recovery rate and collect 2mL for each volumes. Finally, regenerate column by running 20 mL NanoPure water through the column to regenerate it.

- **SiO_2 and Y_2O_3**

To condition the chromatography bed, 5 times of bed volume buffer A (50mM Phosphate Buffer and 50mM $(NH_4)_2SO_4$), 10mL was run through the column using a syringe pump flow rate of 1mL/min to ensure the column reached equilibrium. To support the hypothesis for this study, 10μL of 100ppm metal oxides were injected into the column. After injecting, the flow rate was started at 5ml/min. Elute nanoparticles through the column and reduces hydrophobic interaction by decreasing phosphate buffer concentrations in step manner from 50mM, 40mM, 30mM, 20mM, 10mM, to 0mM, and collect 3mL for each salt concentration, then 3mL 80% ethanol as last stage to reach 100% recovery rate. Finally, regenerate column by running 20 mL NanoPure water through the column to regenerate it.

C. PEGylated-SiO_2

To condition the chromatography bed, 5 times of bed volume buffer A (50mM Phosphate Buffer and 50mM $(NH_4)_2SO_4$), 10mL was run through the column using a syringe pump flow rate of 1mL/min to ensure the column reached equilibrium. To support the hypothesis for this study, 10μL of 100ppm PEGylated-SiO_2 were injected into the column. After injecting, the flow rate was started at 5ml/min. Elute nanoparticles through the

column and reduces hydrophobic interaction by decreasing phosphate buffer concentrations in step manner from 50mM, 40mM, 30mM, 20mM, 10mM, to 0mM and collect 3mL for each salt concentration, then 3mL 80% ethanol as last stage to reach 100% recovery rate. Finally, regenerate column by running 20 mL NanoPure water through the column to regenerate it.

3.1.6 Data Collection

The data of CNC was analyzed by Nanoparticles Tracking Analysis (NTA) – NanoSight 500 (NS500) was used to visualize and analyze particles in liquids, from 10-2000nm, that relates the rate of Brownian motion to particle size track. NS500 was purchased from NanoSight Ltd (Amesbury, UK).

Dynamic Light Scattering (DLS) (Zetasizer, Malvern Instruments Ltd. Worcestershire, UK) was used to assess the hydrodynamic diameter of nanoparticles and agglomerates. The attenuator index was adjusted to 11 to get 100% transmission and measurement position at 6mm - the center of the cuvette. Count rate (per second) in DLS was used to determine the quality of sample by detecting the sample stability over time, and used to set up parameters like attenuator. A calibration curve of the nanoparticles specific count rate under different concentration was generated to calculate eluent nanoparticle concentrations by measuring count rate.

3.1.7 Data Analysis

MATLAB (Natick, Massachusetts) was used to convert count rate to concentration. Statistical analyses were conducted by SigmaStat (San Jose, CA). One way ANOVA was used to determine the concentration variance of each volume, where showed significant when $p < 0.05$.

3.2 Dye Adsorption

3.2.1 Materials

Rose Bengal (hydrophobic dye, 85%, high purity, biological stain, absorbance: 547.2nm) and Nile Blue (hydrophilic dye, pure, certified, MW 732.87, absorbance: 635nm) were purchased from Acros Organics (New Jersey, USA). Gold nanorod (wavelength: 550nm, axial diameter 25nm, store at 4°C) were purchased from Sterm Chemical. C_6H_5OH (Phenol, ACS, 99+%, crystalline) was purchased from Alfa Aesar (Ward Hill, MA). Na_2HPO_4 (sodium phosphate, dibasic, anhydrous, granular, 99.1%) is from Macron Chemicals (Center Valley, PA) and NaH_2PO_4 (sodium phosphate, monobasic, anhydrous, 99%) was purchased from Fisher Scientific (Fair Lawn, NJ). NanoPure water was generated from a Milli-Q ultra-pure system with a resistivity 18MΩcm.

3.2.2 Stock Solution Preparation

Stock solution was prepared by dissolving 28.392g of Na_2HPO_4 and 23.996g of NaH_2PO_4 separately in 1 liter NanoPure to prepare 0.2M salt solution. Next, 160 ml NaH_2PO_4 solution and 840 ml Na_2HPO_4 solution were mixed together to reach final pH of 7.5. Finally, 750ml of NanoPure water was used to dilute the phosphate buffer to 1 liter 50mM buffer as stock buffer solution.

Rose Bengal and Nile Blue dry powder 40mg were added to l liter NanoPure water, and stored in an amber glass bottle to protect from light.

3.2.3 Experiment Procedure

Gold nanorods were prepared in three increasing concentration: 5mg/L, 10mg/L, and 15mg/L. Gold nanorods were incubated in 50mM phosphate buffer with 40mg/L dye solution to reach final concentration 20mg/L, and were kept in the dark environment for 3 hours. After three hours, samples were centrifuged (4500g) for 1.5 hours to separate bound and unbound dye. The Partitioning Quotient (PQ) was determined and plotted against total hydrophobic surface area to know their hydrophobicity.

3.2.4 Data Collection

SpectraMax M2 (Sunnyvale, CA) was used to measure the absorbance and quantify the amount of dye in solution. Calibration curves were generated for Rose Bengal (543nm) and Nile Blue (635nm) at different nanoparticle concentrations and analyzed by SpectraMax. Absorbance values were used to calculate the amount of dye adsorbed on the nanoparticles.

3.2.5 Data Analysis

Statistical analyses were conducted by SigmaStat (San Jose, CA). One way ANOVA was used to determine the separation efficiency of bound and unbound dye onto gold nanorods after centrifuge, where showed significant when $p<0.05$. The PQ value was calculated from Eqn. (6) and Eqn. (7). PQ was plotted versus the total surface area and linear regression was used to obtain the slope of the regression line.

Chapter 4: Result

4.1 HIC

As mention in Chapter 2.2.3, there are a lot of factors can affect the performance of HIC, such as salt buffer, buffer pH, elution rate and packed volume. The reason for using metal oxides as sample materials is due to their relative hydrophobicity can be described by their isoelectric point and can correlate to chromatographs. Hydrophobic property of CNC is pH dependent, and thus can easily compare the hydrophobicity with altering their pH.

4.1.1 Optimizing the HIC assay for Nanomaterial Evaluations

In order to optimize the performance of HIC and characterize the hydrophobicity of metal oxides rapidly, the presence of wash step, salt selection, salt concentration, elution rate, elution buffer pH and packed volume would be covered in this section.

A. Washing
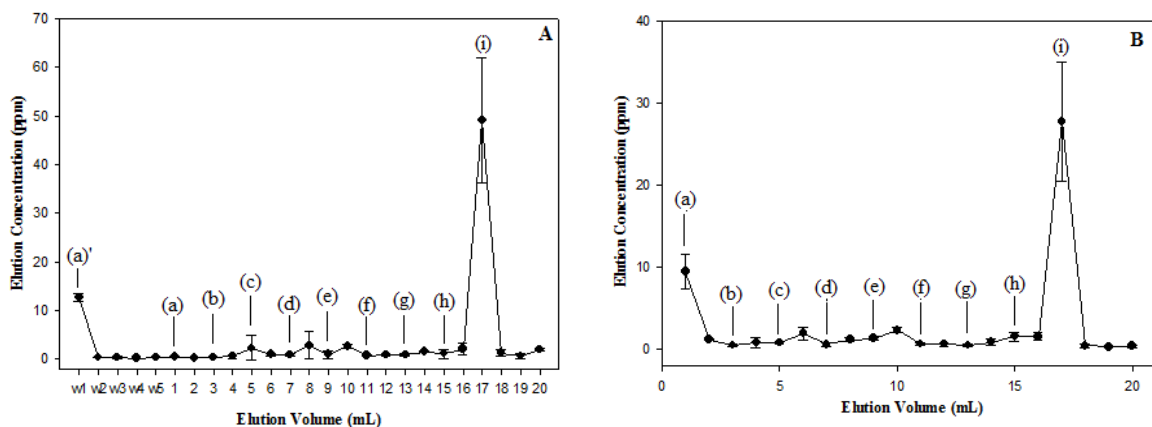
Fig 4.1 Chromatographs of aluminum oxide doped silicon oxide (Al_2O_3-SiO_2) on phenyl-sepharose medium: (A) with a wash step and (B) without a wash step. Elution was performed by decreasing $(NH_4)_2SO_4$ concentration from (a) 0.1M, (b) 0.05M, (c) 0.01M, and (d) 0M, followed by (e) 10%, (f) 20%, (g) 40%, (h) 80%, and (i) 100% ethanol at flow rate of 10ml/min. ((a)' is wash step)

In protein separation, various kinds of proteins with different hydrophobicity run through the packed column, thus there is a need to wash unbound proteins out of column. Since only one type of nanomaterial was run through columns at a time, the wash step can be taken out saving time in running the assay. In Fig 4.1, Al_2O_3 was run through the column and compared the need of wash step and showed that recovery rate was 29.3% and 27.72% for washing and not respectively which indicates no significant difference between with or without the wash step. Running HIC in this protocol without a wash step can shorten the operation time.

B. Salt Selection
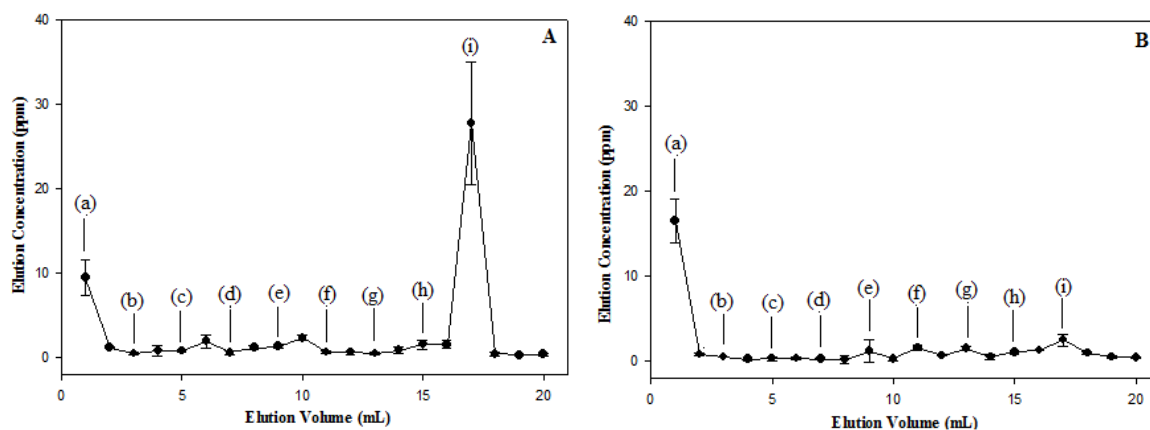
Fig 4.2 Chromatographs of aluminum oxide doped silicon oxide (Al_2O_3-SiO_2) for different mobile phase on phenyl-sepharose medium. Elution buffer was changed from (A) $(NH_4)_2SO_4$ to (B) $MgCl_2$. Elution was performed by decreasing salt concentration from (a) 0.1M, (b) 0.05M, (c) 0.01M, and (d) 0M, followed by (e) 10%, (f) 20%, (g) 40%, (h) 80%, and (i) 100% ethanol at flow rate of 10ml/min.

The recovery rate for using $(NH_4)_2SO_4$ as elution buffer to measure hydrophobicity of nanoparticles was 27.72% and this may result from $(NH_4)_2SO_4$ in Hofmeister series is the strongest salt to promote the salting-out effect (Fig 2.2.5). Also, phenyl ligands were used as stationary phase in this assay and may lead to extremely strong hydrophobic interaction making it is hard for nanoparticles to elute. Thus, applying $MgCl_2$ which

caused less salting out effect in the Hofmeister series as elution buffer to instead of $(NH_4)_2SO_4$. However, the recovery rate of using $MgCl_2$ as mobile phase was less than $(NH_4)_2SO_4$, it was only 15.81%. This low recovery rate was likely due to electrostatic interactions between cations of salt solution and pi bonds of phenyl ligand. The more positively charged cations lead to larger cation-pi interaction, increasing the interaction between ligands and nanoparticles and make the retention longer.

C. Bed Volume
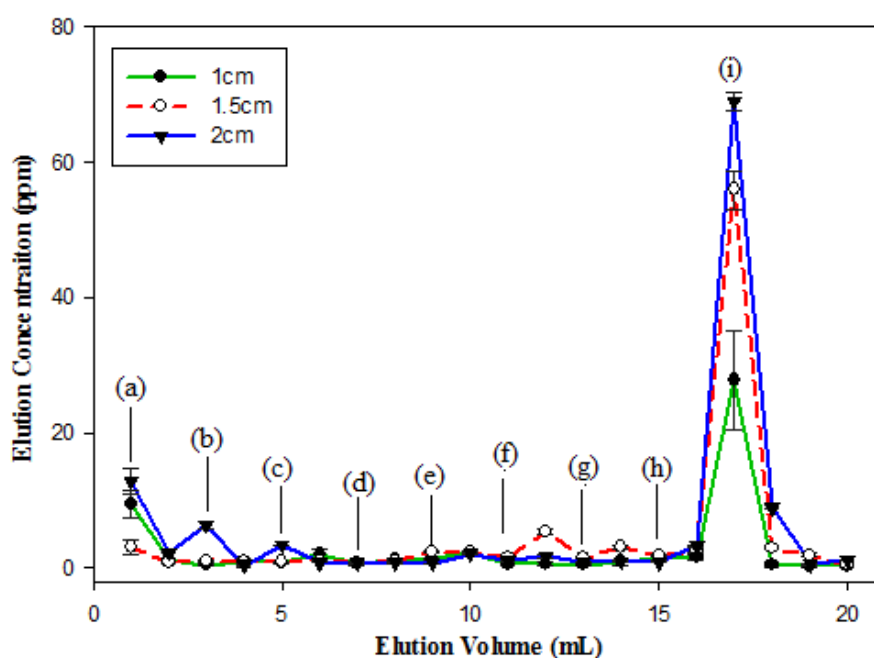
Fig 4.3 Chromatographs of aluminum oxide doped silicon oxide ($Al2O_3$-SiO_2) with increasing volume of phenyl-sepharose medium. Elution was performed by decreasing salt concentration from (a) 0.1M, (b) 0.05M, (c) 0.01M, and (d) 0M, followed by (e) 10%, (f) 20%, (g) 40%, (h) 80%, and (i) 100% ethanol at flow rate of 10ml/min.

The recovery rate for running Al_2O_3-SiO_2 through the column was 27.72%. In chromatography, it is hard to get good separation if there is not enough packed medium volume. Thus, by increasing the stationary phase, packed bed volume from 1cm, 1.5cm to 2 cm and it was found that 2cm medium height can achieve twice the recovery rate compared with a 1cm high medium. The recovery for 1.5cm was 44.75% and 2cm was

59.78% after increasing packed bed volume. Hence, from the result we can know that moderate high packed volume is needful to optimize the performance of HIC.

D. Elution Rate

According to Fig A.2.1 and Fig A.2.2, the calibration curve for Al_2O_3-SiO_2 is 3rd order dynamic curve and induce 7% to 8% function transfer error. This meant the low recovery rate we obtained had some degree of error and need use other material to instead of it. The calibration curve for SiO_2 is the 2nd order (Fig A.2.3) which caused less function transfer error and more likely to be adopted as sample materials due to it was simpler than Al_2O_3-SiO_2.
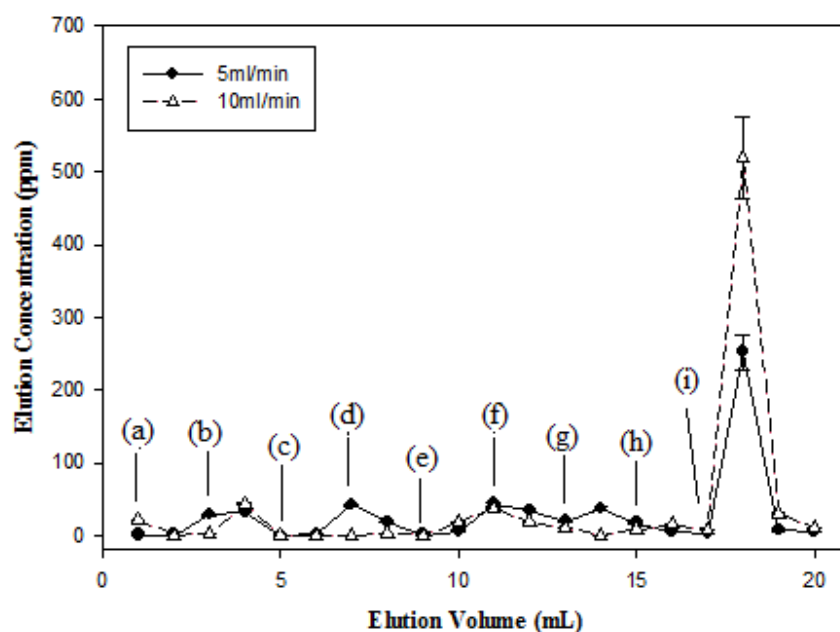
Fig 4.4 Chromatographs of silicon dioxide (SiO_2) with different elution rate on phenyl-sepharose medium. Elution was performed by decreasing salt concentration from (a) 0.1M, (b) 0.05M, (c) 0.01M, and (d) 0M, followed by (e) 10%, (f) 20%, (g) 40%, (h) 80%, and (i) 100% ethanol at flow rate of 10ml/min.

Recovery rate decreased with a decrease in elution rate. SiO_2 had a recovery rate at a 10ml/min flow rate that was 297%. Hence, the elution rate was decreased from 10ml/min

to 5 ml/min, but the recovery was still greater than 100%, it was 220%. This may due to the high salt concentration to cause nanoparticle agglomeration. A recent study showed that the critical salt concentration for nanoparticles is 100mM (Jiang, Oberdörster et al. 2009). High salt concentrations can cause nanoparticles to agglomerate and make DLS measurements skewed to give a proper count rate. Thus, the recovery rate appears to be over 100%.

E. pH Control

As discussed in Chapter 2.2.3, pH control is one of the key factors that influence column performance. The IEP information which I based on to predict the hydrophobicity of metal oxides was controlled at pH7.4 (Fig B.1). In this method, phosphate buffer was used as an elution buffer and pH was increased from 5.6 to 7.4.
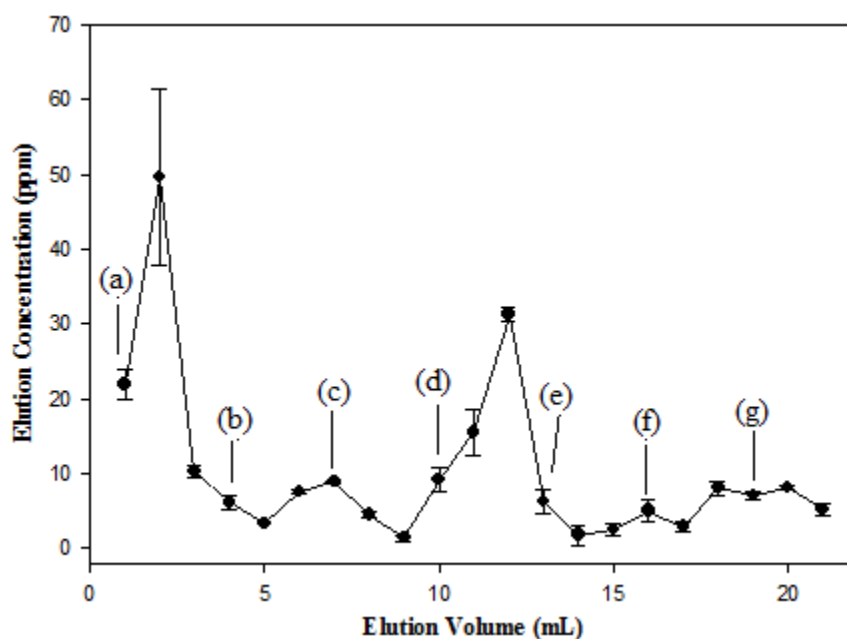
Fig 4.5 Chromatographs of silicon dioxide (SiO_2) on phenyl-sepharose medium. Elution was performed by decreasing phosphate buffer concentration from (a) 50mM, (b) 40mM, (c) 30mM, (d) 20mM, (e) 10mM to (f) 0mM, followed by (g) 80% ethanol at flow rate of 5ml/min.

Based on the theoretic chromatograph of nanoparticles (Fig 1.4.1), hydrophilic nanoparticles have less hydrophobic interaction with ligands and show an earlier elution peak on the chromatograph when compared with hydrophobic nanoparticles. From the result of Fig 4.5, hypothesis was supported. The hydrophobicity of SiO_2 can be described by their IEP that the IEP of SiO_2 is 1.0 at pH7.4 (Chapter 1.4.1). SiO_2 was surrounded by OH^- group, formed hydrogen bond with water and thus SiO_2 is hydrophilic nanoparticles. The maximum elution peak of SiO_2 was in earlier stage of HIC and showed their hydrophilicity.

4.1.2 Effect of pH on Nanomaterial Hydrophobicity

As discussed earlier in Chapter1.4.1, pH is an important parameter not only in optimizing the performance of HIC, but also for determining the nanoparticle hydrophobicity. The hydrophobicity of CNC and metal oxides are covered in this section.

A. Varying pH: Carboxylated Nanocrystalline Cellulose (CNC)
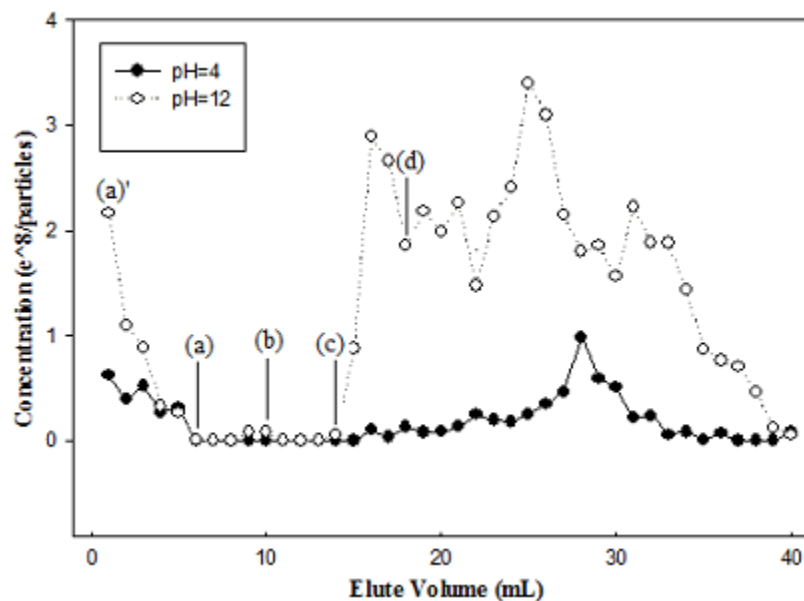
Fig 4.6 Chromatographs of carboxylated nanocrystalline cellulose (CNC) at eluted through phenyl-sepharose medium. Elution was performed by decreasing salt concentration from (a) 2M, (b) 1.5M, (c) 0.5M, and (d) 0M at flow rate of 1ml/min.

Using CNC as test materials are due to their hydrophobicity is pH dependent; CNC is hydrophobic in a low pH environment and hydrophilic in high pH environment. Meanwhile, we can know whether HIC can be used to measure the hydrophobicity of nanoparticles or not. From Fig 4.6 we can know that the elution amount of CNC at pH=12 is more than pH=4 and this informed us that CNC is hydrophobic in low pH and have strong interaction with hydrophobic ligands, longer retention time and thus have less elution than high pH hydrophilic CNC.

B. Isoelectric Point: SiO_2 vs. Y_2O_3
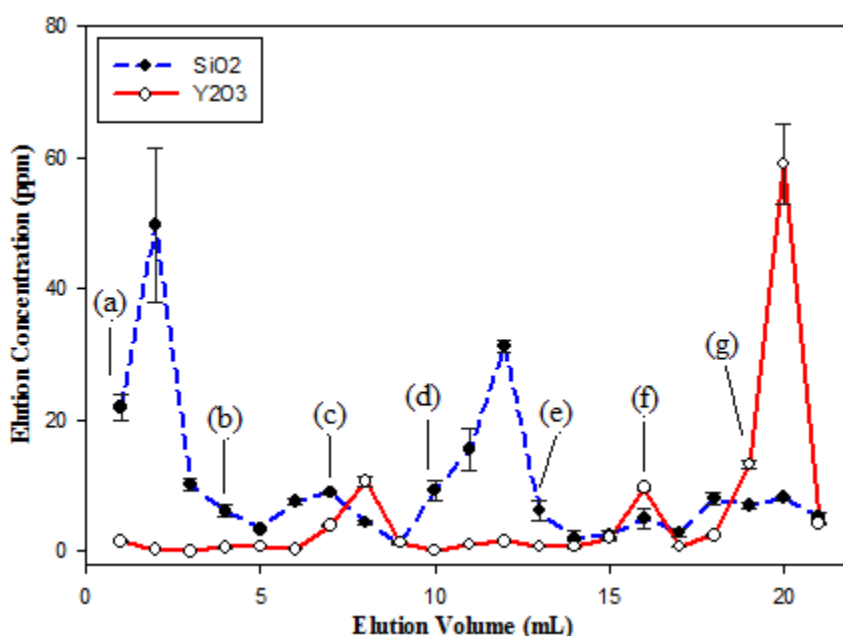
Fig 4.7 Chromatographs of silicon dioxide (SiO_2) and yttrium oxide (Y_2O_3) on phenyl-sepharose medium. Elution was performed by decreasing phosphate buffer concentration from (a) 50mM, (b) 40mM, (c) 30mM, (d) 20mM, (e) 10mM to (f) 0mM, followed by (g) 80% ethanol at flow rate of 5ml/min.

Fig 4.7 showed the relative hydrophobicity of SiO_2 and Y_2O_3 that supported hypotheses in Chapter 1.4.1. The IEP of Y_2O_3 is 9.7 at pH7.4 which present it is a relative hydrophobic metal oxide when compared with hydrophilic SiO_2 whose IEP is 1.0 at pH7.4. Thus, the maximum elution peak of Y_2O_3 was expected to be later in the

chromatographs than hydrophilic SiO_2, due to hydrophobic Y_2O_3 have strong hydrophobic interactions with the hydrophobic phenyl ligands and thus retained longer in the column. Fig 4.7 shows the maximum peak for Y_2O_3 was at 20th volumes with a 104% recovery rate and maximum peak for SiO_2 was in 2nd volumes with a 93.75% recovery rate.

4.1.3 Effect of Surface Chemistry on Nanomaterial Hydrophobicity: SiO_2 vs. PEG-SiO_2
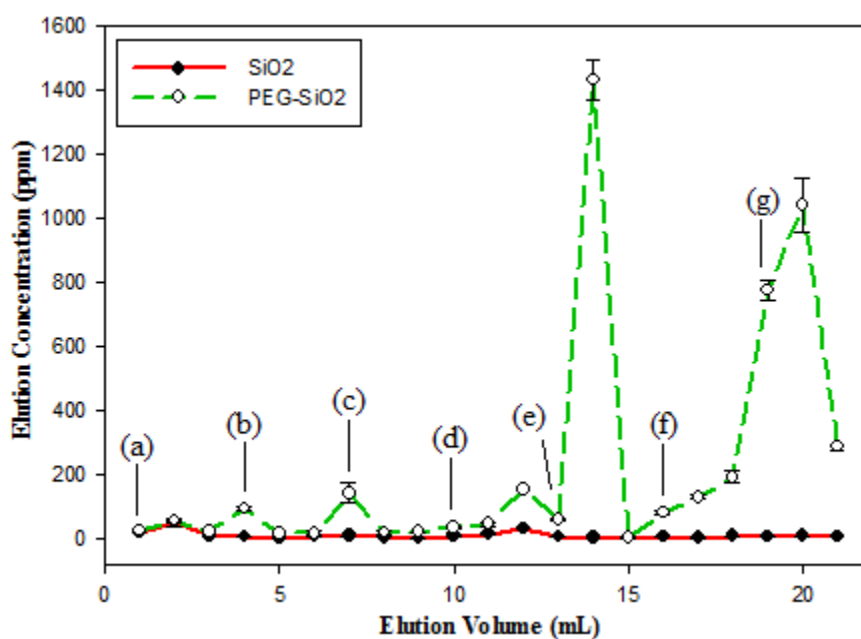
Fig 4.8 Chromatographs of silicon dioxide (SiO_2) and PEGylated silicon oxide (PEGylated-SiO_2) on phenyl-sepharose medium. Elution was performed by decreasing phosphate buffer concentration from (a) 50mM, (b) 40mM, (c) 30mM, (d) 20mM, (e) 10mM to (f) 0mM, followed by (g) 80% ethanol at flow rate of 5ml/min.

From Fig 4.8, PEGylated- SiO_2 showed much more eluent when compared to SiO_2. In fact, the recovery rate of PEGylated- SiO_2 was1876% and it was 18 times larger than the recovery rate of SiO_2. PEGylated- SiO_2 is a very hydrophilic chemical polymer and is soluble in water, benzene, and ethanol and not compatible with chemicals such as hexane or diethyl ether. Thus concern was raised about the potential breakdown of the column.

PEG may dissolve phenyl ligand of stationary phase which lead to recovery rate of PEGylated- SiO_2 that was 1876%. This result also showed that surface coatings dominated the hydrophobicity of nanoparticles, not their core.

4.2 Dye Adsorption
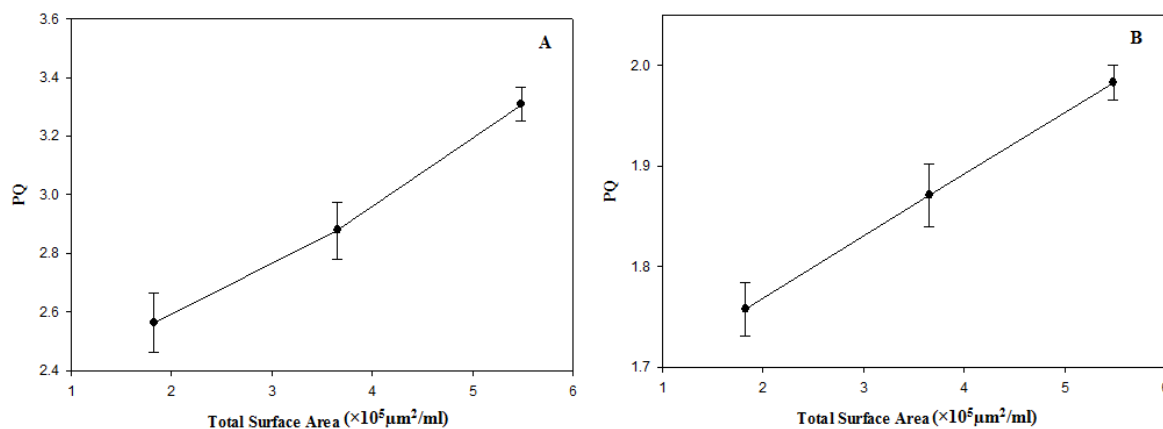
Fig 4.9 (A) Hydrophobicity measured by adsorption Rose Bengal onto gold nanorods surface (slope=0.3729) (B) Hydrophilicity measured by adsorption Nile Blue onto gold nanorods surface (slope=0.1147)

Dye adsorption was used to test the hydrophobicity of gold nanorods in Fig 4.9. The amount of hydrophobic Rose Bengal dye adsorbed onto nanoparticles increased with increased surface area (Fig 4.9 (A)); the amount of hydrophilic Nile Blue dye adsorbed onto nanoparticles increased as increasing surface area (Fig 4.9 (B)). The use of hydrophobic and hydrophilic dye can show a continuum from hydrophobic to hydrophilic. In both of the Fig 4.9 (A) and Fig 4.9 (B) showed the linearity of dye adsorption response and which means we can calculate PQ based on total surface area of nanoparticles. Normalizing the PQ for total surface area and plot the value of the ratio of Rose Bengal to Nile Blue, we can know the relative hydrophobicity of nanoparticles (Fig 4.10).
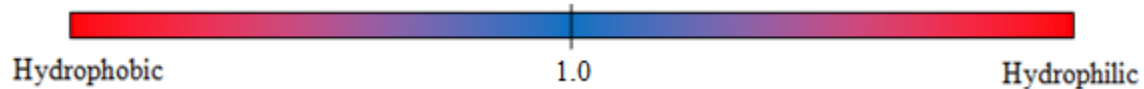
Fig 4.10 The index bar for the relative hydrophobicity/hydrophilicity from the ratio of hydrophobic slope to hydrophilic slope

If the ratio larger than 1.0, it would be hydrophobic; if the ratio smaller than 1.0, it would be hydrophilic and as far from 1.0 the nanoparticles would be more hydrophobic or hydrophilic. The ratio for gold nanorod is 3.25 and showed hydrophobic property.

Chapter 5: Discussion

Due to dynamic nature of nanoparticles, their hydrophobicity cannot be measured by contact angle because they form agglomeration and continuously shift at the interface of solid/liquid and vapor/liquid. Partition coefficient also has problem in measuring nanoparticle hydrophobicity because nanoparticles cannot in solution they only disperse, thus they cannot reach an equilibrium state between water and octanol phase. They continuously shift their distribution, forming agglomeration and accumulation at interface of octanol/water. Hence, the need for developing methods to characterize their hydrophobicity is urgent. The objective of this study was to solve the problems arised by traditional methods to measure the hydrophobicity of engineered nanoparticles. There are two methods – HIC and dye adsorption was assessed in this study.

5.1 Hydrophobic Interaction Chromatography (HIC)

5.1.1 Overall Viability and Promise of HIC Technique

Although hydrophobic interaction chromatography has been widely used in protein separation and purification for a long while, related literature about application in measuring relative hydrophobicity of nanoparticles has not yet matured. The parameters like elution buffer pH, packed volume and buffer selection which can optimize the performance of HIC has been discussed in this study (Chapter 4.1). However, HIC cannot use to measure complicated nanomaterials and extremely hydrophilic nanoparticles such as PEGylated nanoparticles. As more and more sophisticated nanomaterials were designed, HIC may not a promising method to look at.

5.1.2 Nanomaterial Hydrophobicity

HIC results supported that relative hydrophobicity of CNC is pH dependent (Chapter 4.1.2). CNC is hydrophilic in a high pH environment and hydrophobic in a low pH environment. For the metal oxides (SiO_2 and Y_2O_3), their relative hydrophobicity was predicted by their isoelectric point. Y_2O_3 has higher isoelectric point 9.7 than SiO_2 1.0 at pH7.4, and thus show Y_2O_3 higher hydrophobicity than SiO_2. HIC results also supported the prediction that hydrophilic SiO_2 would elute faster than hydrophobic Y_2O_3 (Chapter

1.4.1). The surface coating of nanoparticles dominated hydrophobicity of nanoparticles. PEGylated-SiO_2 showed higher hydrophilicity than SiO_2, because PEG ligand onto surface of PEGylated-SiO_2 dissolved the phenyl-ligand of medium and SiO_2 didn't (Fig 4.8). From Fig 4.7 and Fig 4.8, we can compare the hydrophobicity of metal oxides that Y_2O_3 is the most hydrophobic metal oxides among the three, than SiO_2 and then PEGylated-SiO_2.

5.1.3 HIC Method Assessment

The importance of choosing proper parameters such as salt selection, salt concentration, and salt pH value, volume of packed bed and elution rate to measure relative hydrophobicity of nanoparticles have been discussed in this study (Chapter 4.1). Since salt solution cause nanoparticles agglomeration, the selection of using phosphate buffer as mobile phase was found to reduce the instability of nanoparticles size during HIC process. As literatures proposed, 100mM is a critical concentration for nanoparticles forming agglomeration (Hjerten 1973; Lienqueo, Mahn et al. 2007). Controlled pH at a proper values is a critical in this protocol and the data information about isoelectric point and zeta potential is measured at pH 7.4 is in Appendix B (Liu, Zhang et al. 2013). It is hard to reach ideal separation if packed volume is not enough. The recovery rate is twice larger after increasing stationary phase two times in this research. Elution rate also should be controlled at proper rate, too slow elution rate would lead too much hydrophobic interaction and make nanoparticles hard to elute; too fast elution rate would cause not enough hydrophobic interaction and hard to collect the elute nanoparticles. As discussed in Fig 4.8, PEGylated-SiO_2 dissolved the phenyl-ligand of medium and degraded the performance of HIC. Thus, HIC may be more applicable for simple nanoparticles like metal oxides and have more limitations for more sophisticated nanoparticles. Although columns are reusable, in order to avoid the unseen degradation or retention of nanoparticles, column should be replaced when measuring new materials or after using three times.

5.1.4 Limitations of HIC for Nanomaterial Analysis

HIC could not be used with hydrophilic materials such as PEGylated-SiO_2, which dissolved the ligands and degraded performance of HIC. The recovery rate of nanoparticles is hard to reach 100% and thus decrease the feasibility of HIC method. Besides, it may have issue when measuring the hydrophobicity of non-spherical nanoparticles. The orientation and axis-ratio of nanoparticles may have different degree of hydrophobic interaction with the ligands, cause different degree of retention and make HIC hard to measure the hydrophobicity of non-spherical nanoparticles.

5.1.5 Paths Forward to Overcome Limitations

Using the hydrophilicity that less than PEGylated-SiO_2 or simple nanoparticles to run through the HIC to prevent column from degradation. The reason for could not obtain 100% recovery rate is that nanoparticles is sensitive to the presence of salt buffer, easily to form agglomeration and may cause the measurement which measured by DLS have some inaccuracy. Thus, a study proposed that adding some polyelectrolyte to increase stability of eluent by inducing electrostatic repulsion and decrease the degree of agglomeration which raised from running salt buffer as elution buffer to improve the recovery rate (Jiang, Oberdörster et al. 2009).

5.2 Dye Adsorption
5.2.1 Overall Viability and Promise of Dye Adsorption Technique

Start with this dye adsorption may be is a feasible and more promising method to measure the relative hydrophobicity of engineered nanoparticles. Surface hydrophobicity of nanoparticles can be quantified by using Rose Bengal partitioning method. The slope is an index for determining surface hydrophobicity of nanoparticles. The higher the slope, the more hydrophobic is the surface of the nanoparticle. The hydrophilic Nile Blue dye is also used in this study, to show a continuum from hydrophobicity to hydrophilicity. Thus, the ratio of hydrophobic to hydrophilic was calculated and can be an index to show the hydrophobicity of nanoparticles.

5.2.2 Nanomaterial Hydrophobicity

Hydrophobicity of gold nanorods was qualified and quantified using the dye adsorption method in this study and the ratio of Rose Bengal to Nile Blue is 3.25 which can assess the hydrophobicity of gold nanorods.

5.2.3 Dye Adsorption Method Assessment

Dye adsorption used hydrophobic Rose Bengal dye and hydrophilic Nile Blue dye to show the continuum from hydrophobic to hydrophilic. Thus, the hydrophobicity of nanoparticles can be quantified, easily to compare the hydrophobicity of nanoparticles from an index bar (Fig 4.10). However, the presence of surfactant should be avoided due to it induced inaccuracy to this measurement.

5.2.4 Limitations of Dye Adsorption for Nanomaterial Analysis

The presence of CTAB, a kind of surfactant used to assist dispersion of gold nanorods, may distort the degree of hydrophobicity of gold nanorods. Besides, the cationic hydrophilic dye may cause electrostatic interaction with negatively charged nanoparticles and induce inaccuracy for the measurement.

5.2.5 Paths Forward to Overcome Limitations

The issue raised by the presence of CTAB can be overcome through simple dispersed nanoparticles, for example, the nanoparticles only dispersed in water. The inaccurate measurement raised by electrostatic interaction between cationic hydrophilic dye and negative nanoparticles can be solved by using neutral charged hydrophilic dye, such as Magenta dye.

5.3 Comparison of HIC and Dye Adsorption for Determining the Relative Hydrophobicity of Nanomaterials

Dye adsorption showed a continuum form the hydrophobicity to hydrophilicity by using Rose Bengal and Nile Blue, and can be quantified to a ratio value (Rose Bengal: Nile Blue), then qualified their hydrophobicity. However, in HIC, the relative

hydrophobicity/hydrophilicity can be determined by the order of elution, cannot be quantified to a number and thus less accuracy than dye adsorption. SpectraMax, which is the equipment used in collecting dye adsorption data, can get all of the data information quickly; DLS only can read individual data at a time. Comparing their preparation procedure, HIC column need to be packed well and make sure there are no voids inside the column, if there are any voids inside the column then the column should be repacked and this took a lot time. In HIC, care should be taken on the degradation of column, accumulation of nanoparticles and voids which raised by running ethanol, and these reasons may induce inaccuracy when measuring nanoparticle hydrophobicity. To summarize, dye adsorption would be a more promising method.

Chapter 6: Conclusions

6.1 Intellectual Contributions

From this study, we can know the hydrophobicity of CNC is pH dependent (Chapter 1.4.1). The hydrophobicity of metal oxides can be described from their IEP at a given pH (Chapter 1.4.1). The control of elution buffer pH, buffer selection, packed bed volume, and elution rate is all important for optimizing the column performance (Chapter 2.2.3& Chapter 4.1). HIC can be used to measure the hydrophobicity of simple nanoparticles (Chapter 5.1). Coating dominated the hydrophobicity of nanoparticles, not the core. PEG-SiO_2 degraded the performance of HIC and SiO_2 did not (Fig 4.8). Dye adsorption can show continuum form hydrophobicity to hydrophilicity, be quantified to a ratio and then is a feasible method (Chapter 4.2). The presence of surfactant affected the hydrophobicity of nanoparticles. CTAB assisted the dispersion of gold nanorods, but also distorted the hydrophobicity of gold nanorods (Chapter 5.2). Comparing HIC and dye adsorption, the cost of HIC and dye adsorption is same if using phenyl sepharose as stationary phase. Cost of HIC will be lot more expensive if using butyl sepharose. For time involving, HIC need spend a lot of time on preparing, operating and analyzing.

6.2 Recommendations for Future Studies

For HIC study, the packed bed volume was limited to 2ml inside 2.5ml column. Future study can use higher volume column and increase packed bed volume to increase the nanoparticle separation. There are four parts would be covered in future studies of dye adsorption. First, in material selection, should focus on nanomaterials can disperse without surfactant to obtain more accurate result. Second, due to the hydrophobicity of metal oxides can be predicted by their isoelectric point, thus metal oxides can be applied in dye adsorption and correlate the predicted hydrophobicity data with dye adsorption result. Third, dye adsorption can be extended to measure hydrophobicity of nanoparticles from hydrophilic environment to lipophilic environment. For very hydrophobic materials, they cannot run with Rose Bengal because they cannot go into dispersion. Therefore, we can conduct and extend dye adsorption assay in lipophilic environment to apply this method to hydrophobic nanomaterials. Fourth, testing the sensitivity of dye adsorption by

exposure the nanoparticles under various dye concentrations to know the relation between dye concentration and adsorption.

References

Alemdaroglu, F. E., N. C. Alemdaroglu, et al. (2008). "Cellular uptake of DNA block copolymer micelles with different shapes." Macromolecular Rapid Communications **29**(4): 326-329.

Arvizo, R. R., O. R. Miranda, et al. (2010). "Effect of nanoparticle surface charge at the plasma membrane and beyond." Nano Lett **10**(7): 2543-2548.

Cassie, A. B. D. (1948). "Contact angles." Discussions of the Faraday Society **3**: 11-16.

Cassie, A. B. D. and S. Baxter (1944). "Wettability of porous surfaces." Transactions of the Faraday Society **40**: 546-551.

Chen, K. L. and M. Elimelech (2007). "Influence of humic acid on the aggregation kinetics of fullerene (C60) nanoparticles in monovalent and divalent electrolyte solutions." J Colloid Interface Sci **309**(1): 126-134.

Chithrani, B. D., A. A. Ghazani, et al. (2006). "Determining the size and shape dependence of gold nanoparticles uptake into mammalian cells." Nano letters **6**(4): 662-668.

Chiu, Y. L., Y. C. Ho, et al. (2010). "The characteristics, cellular uptake and intracellular trafficking of nanoparticles made of hydrophobically-modified chitosan." J Control Release **146**(1): 152-159.

Christian, P., F. Von der Kammer, et al. (2008). "Nanoparticles: structure, properties, preparation and behavior in environment media." Ecotoxicology **17**(5): 326-343.

Cronin, M. T. D. (2006). "The Role of Hydrophobicity in Toxicity Prediction." Current Computer-Aided Drug Design **2**(4): 405-413.

D'Addio, S. M., W. Saad, et al. (2012). "Effects of block copolymer properties on nanocarrier protection from in vivo clearance." J Control Release **162**(1): 208-217.

Darlington, T., A. Neigh, et al. (2009). "Nanoparticle Characteristics Affecting Environmental Fate And Transport Through Soil." **28**(6): 1191-1199.

De Jong, W. H., W. I. Hagens, et al. (2008). "Particle size-dependent organ distribution of gold nanoparticles after intravenous administration." Biomaterials **29**(12): 1912-1919.

Doktorovova, S., R. Shegokar, et al. (2012). "Modified Rose Bengal assay for surface hydrophobicity evaluation of cationic solid lipid nanoparticles (cSLN)." Eur J Pharm Sci **45**(5): 606-612.

Domingos, R. F., N. Tufenkji, et al. (2009). "Aggregation of titanium dioxide nanoparticles Role of a fulvic acid." Environmental science & technology **43**(5): 1282-1286.

Elimelech, M., J. Gregory, et al. (1995). "Pore Scale Simulation of Colloid Deposition."

Gao, H., J. Xiong, et al. (2013). "In vivo biodistribution of mixed shell micelles with tunable hydrophilic/hydrophobic surface." Biomacromolecules **14**(2): 460-467.

Geng, Y., P. Dalhaimer, et al. (2007). "Shape effects of filaments versus spherical particles in flow and drug delivery." Nat Nanotechnol **2**(4): 249-255.

Goodman, C. M., C. D. McCusker, et al. (2004). "Toxicity of Gold Nanoparticles Functionalized with Cationic and Anionic Side Chains." Bioconjugate Chem. **15**: 897-900.

Gosens, I., J. A. Post, et al. (2010). "Impact of agglomeration state of nano- and submicron sized gold particles on pulmonary inflammation." Part Fibre Toxicol **7**(1): 37.

Greenwood, R. and K. Kendall (1999). "Selection of suitable dispersants for aqueous suspensions of zr and Ti powders using acoustophoresis." Journal of the European Ceramic Society **19**(4): 479-488.

Gref, R., Y. Minamitake, et al. (1994). "Biodegradable long-circulating polymericnanospheres." Science **263**(5153): 1600-1603.

Hanaor, D., M. Michelazzi, et al. (2012). "The effects of carboxylic acids on the aqueous dispersion and electrophoretic deposition of ZrO2." Journal of the European Ceramic Society **32**(1): 235-244.

He, B., N. A. Patankar, et al. (2003). "Multiple equilibrium droplet shapes and design criterion for rough hydrophobic surfaces." Langmuir **19**: 4999-5003.

Hjertén, S., J. Rosengren, et al. (1974). "Hydrophobic interaction chromatography: The synthesis and the use of some alkyl and aryl derivatives of agarose." Journal of Chromatography A **101**(2): 281-288.

Hjerten, S. (1973). "Some general aspects of hydrophobic interaction chromatography." Journal of Chromatography **87**(2): 325-331.

Hofstee, B. H. J. (1975). "Accessible hydrophobic groups of native proteins." Biochemical and biophysical research communications **63**(3): 618-624.

Hoshino, A., K. Fujioka, et al. (2004). "Physicochemical properties and cellular toxicity of nanocrystal quantum dots depend on their surface modification." Nano Letters **4**(11): 2163-2169.

Hotze, E. M., T. Phenrat, et al. (2010). "Nanoparticle Aggregation: Challenges to Understanding Transport and Reactivity in the Environment." Journal of Environment Quality **39**(6): 1909.

Hwang, G., I. S. Ahn, et al. (2012). "Adhesion of nano-sized particles to the surface of bacteria: mechanistic study with the extended DLVO theory." Colloids Surf B Biointerfaces **97**: 138-144.

Hyung, H., J. Fortner, et al. (2007). "Natural organic matter stabilizes carbon nanotubes in the aqueous phase." ENVIRONMENTAL SCIENCE & TECHNOLOGY **41**(1): 179-184.

Jiang, J., G. Oberdörster, et al. (2009). "Characterization of size, surface charge, and agglomeration state of nanoparticle dispersions for toxicological studies." Journal of Nanoparticle Research **11**(1): 77-89.

Karlsson, H. L., J. Gustafsson, et al. (2009). "Size-dependent toxicity of metal oxide particles--a comparison between nano- and micrometer size." Toxicol Lett **188**(2): 112-118.

Kettiger, H., A. Schipanski, et al. (2013). "Engineered nanomaterial uptake and tissue distribution: from cell to organism." Int J Nanomedicine **8**: 3255-3269.

Kim, S. T., K. Saha, et al. (2013). "The Role of Surface Functionality in Determining Nanoparticle Cytotoxicity." Accounts of Chemical Research **46**(3): 681-691.

Lienqueo, M. E., A. Mahn, et al. (2007). "Current insights on protein behaviour in hydrophobic interaction chromatography." J Chromatogr B Analyt Technol Biomed Life Sci **849**(1-2): 53-68.
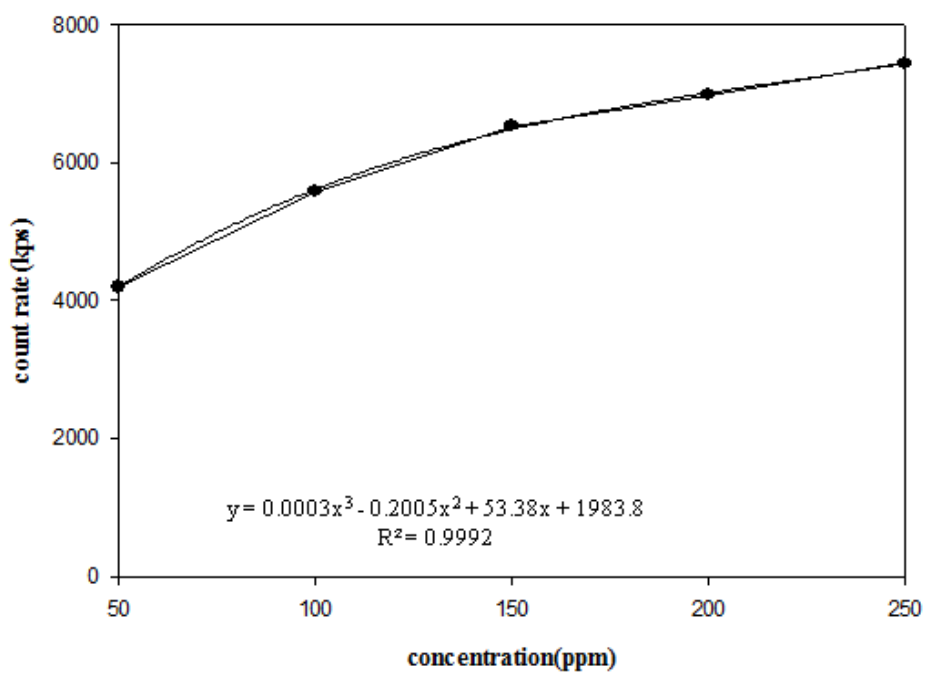
Lim, S. B., A. Banerjee, et al. (2012). "Improvement of drug safety by the use of lipid-based nanocarriers." J Control Release **163**(1): 34-45.

Limbach, L. K., Y. Li, et al. (2005). "Oxide Nanoparticle Uptake in Human Lung Fibroblasts Effects of Particle Size, Agglomeration, and Diffusion at Low Concentrations.pdf>." Environmental science & technology **39**(23): 9370-9376.

Lin, D., X. Tian, et al. (2010). "Fate and Transport of Engineered Nanomaterials in the Environment." Journal of Environment Quality **39**(6): 1896.

Liu, P., R. Guan, et al. (2011). "Toxicity of nano- and micro-sized silver particles in human hepatocyte cell line L02." Journal of Physics: Conference Series **304**: 012036.

Liu, R., H. Y. Zhang, et al. (2013). "Development of structure–activity relationship for metal oxide nanoparticles." Nanoscale **5**: 5644-5653.

Mahn, A. and J. A. Asenjo (2005). "Prediction of protein retention in hydrophobic interaction chromatography." Biotechnol Adv **23**(5): 359-368.

Maynard, A. D., D. B. Warheit, et al. (2011). "The new toxicology of sophisticated materials: nanotoxicology and beyond." Toxicol Sci **120 Suppl 1**: S109-129.

McCarthy, S. A., G. L. Davies, et al. (2012). "Preparation of multifunctional nanoparticles and their assemblies." Nature Protocols **7**(9): 1677-1693.

Meng, H., M. Xue, et al. (2011). "Use of size and a copolymer design feature to improve the biodistribution and the enhanced permeability and retention effect of doxorubicin-loaded mesoporous silica nanoparticles in a murine xenograft tumor model." Acs Nano **5**(5): 4131-4144.

Noel, A., M. Charbonneau, et al. (2013). "Rat pulmonary responses to inhaled nano-TiO2: effect of primary particle size and agglomeration state." Part Fibre Toxicol **10**(1): 48.

Ochoa, J. L. (1978). "Hydrophobic interaction chromatography." Biochimie **60**: 1-15.

Oh, C., Y.-G. Lee, et al. (2009). "Facile synthesis of PEG–silica hybrid particles using one-step sol–gel reaction in aqueous solution." Colloids and Surfaces A: Physicochemical and Engineering Aspects **349**(1-3): 145-150.

Oscarsson, S. and P. Kårsnäs (1998). "Salt-promoted adsorption of proteins onto amphiphilic agarosebased adsorbents II. Effects of salt and salt concentration." Journal of Chromatography A **803**: 83-93.

Pal, S., Y. K. Tak, et al. (2007). "Does the antibacterial activity of silver nanoparticles depend on the shape of the nanoparticle? A study of the Gram-negative bacterium Escherichia coli." Appl Environ Microbiol **73**(6): 1712-1720.

Patankar, N. A. (2003). "On the Modeling of Hydrophobic Contact Angles on Rough Surfaces." Langmuir **19**(4): 1249-1253.

Perry, J. L., K. P. Herlihy, et al. (2011). "PRINT: A Novel Platform Toward Shape and Size Specific NPs Theranostics." Accounts of Chemical Research **44**(10): 990-998.

Porath, J. (1987). "Salting-out adsorption techniques for protein purification." Biopolymers **26**(s0): S193-S204.

Qiu, Y., Y. Liu, et al. (2010). "Surface chemistry and aspect ratio mediated cellular uptake of Au nanorods." Biomaterials **31**(30): 7606-7619.

Queiroz, J. A., C. T. Tomaz, et al. (2001). "Hydrophobic interaction chromatography of proteins." Journal of Biotechnology **87**: 143-159.

Rainer H. Müller, D. R., Martin Lück, Bernd.-R. Paulke (1997). "Influence of fluorescent labelling of polystyrene particles on phagocytic uptake surface hydrophobicity, and plasma protein adsorption." Pharmaceutical Research **14**(1): 18-24.

Schrick, B., B. W. Hydutsky, et al. (2004). "Delivery vehicles for zerovalent metal nanoparticles in soil and groundwater." Chemistry of Materials **16**(11): 2187-2193.

Shvedova, A. A., E. R. Kisin, et al. (2005). "Unusual inflammatory and fibrogenic pulmonary responses to single-walled carbon nanotubes in mice." Am J Physiol Lung Cell Mol Physiol **289**: 698-708.

Sivaraman, B., K. P. Fears, et al. (2009). "Investigation of the Effects of Surface Chemistry and Solution Concentration on the Conformation of Adsorbed Proteins Using an Improved Circular Dichroism Method." Langmuir **25**(5): 3050-3056.

Takahashi, H., Y. Niidome, et al. (2006). "Modification of gold nanorods using phospatidylcholine to reduce cytotoxicity." Langmuir **22**: 2-5.

Wang, S., W. Lu, et al. (2008). "Challenge in understanding size and shape dependent toxicity of gold nanomaterials in human skin keratinocytes." Chem Phys Lett **463**(1-3): 145-149.

Wenzel, R. N. (1936). "Resistance of solid surfaces to wetting by water." Industrial & Engineering Chemistry **28**(8): 988-994.

Wenzel, R. N. (1949). "Surface Roughness and Contact Angle." The Journal of Physical Chemistry **53**(9): 1466-1467.

Wick, P., P. Manser, et al. (2007). "The degree and kind of agglomeration affect carbon nanotube cytotoxicity." Toxicol Lett **168**(2): 121-131.

Xia, F., D. Nagrath, et al. (2004). "Evaluation of selectivity changes in HIC systems using a preferential interaction based analysis." Biotechnol Bioeng **87**(3): 354-363.

Xia, T., M. Kovochich, et al. (2009). "Polyethyleneimine coating enhances the cellular uptake of mesoporous silica nanoparticles." Acs Nano **3**(10): 3273-3286.

Xiao, Y. and M. R. Wiesner (2012). "Characterization of surface hydrophobicity of engineered nanoparticles." J Hazard Mater **215-216**: 146-151.

Zhan, J. J., T. Zheng, et al. (2008). "Transport characteristics of nanoscale functional zerovalent iron_silica composites for in situ remediation of trichloroethylene." Environmental science & technology **42**(23): 8871-8876.

Zhao, X., S. Ng, et al. (2013). "Cytotoxicity of hydroxyapatite nanoparticles is shape and cell dependent." Arch Toxicol **87**(6): 1037-1052.

Zhu, M., G. Nie, et al. (2013). "Physicochemical properties determine nanomaterial cellular uptake, transport and fate." Accounts of Chemical Research **46**(3): 622-631.

Appendix A

A.1 Hydrophobic Interaction Chromatography

$$y = 0.018x^3 - 2.6718x^2 + 172.12x + 51.908$$
$$R^2 = 0.9979$$
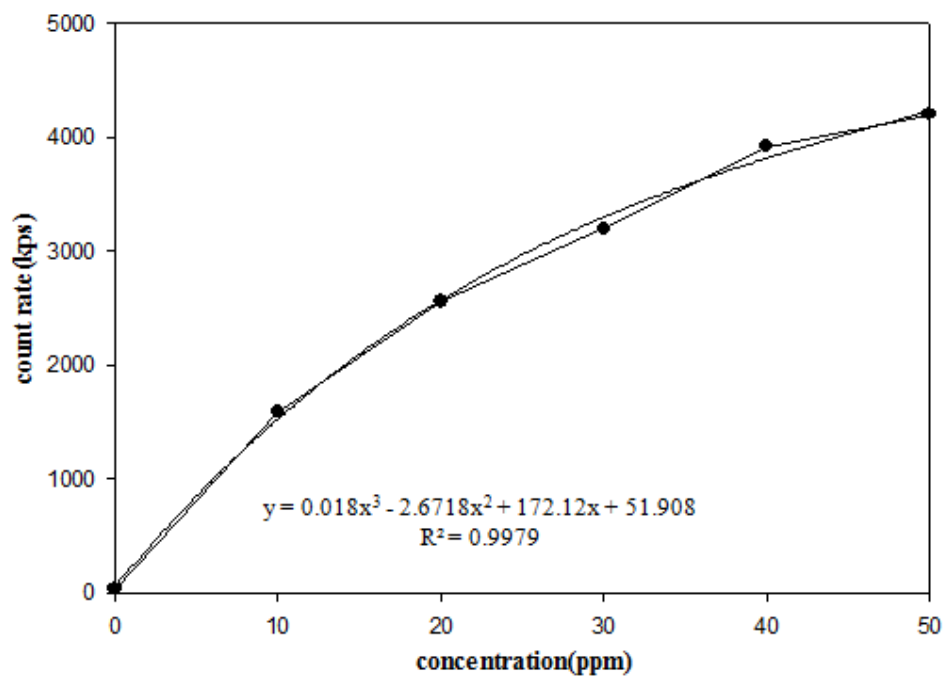
Fig A.1.1 Calibration curve: 0-50ppm Alumina doped silica (Al_2O_3-SiO_2)

$$y = 0.0003x^3 - 0.2005x^2 + 53.38x + 1983.8$$
$$R^2 = 0.9992$$

Fig A.1.2 Calibration curve: 50-250ppm Alumina doped silica (Al_2O_3-SiO_2)
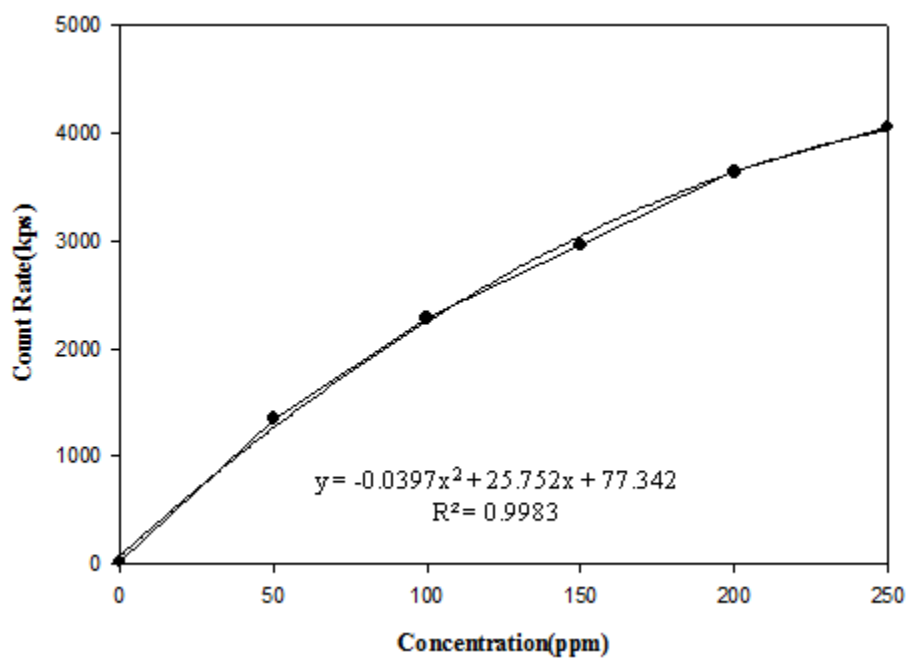
Fig A.1.3 Calibration curve for SiO_2 is the 2nd order
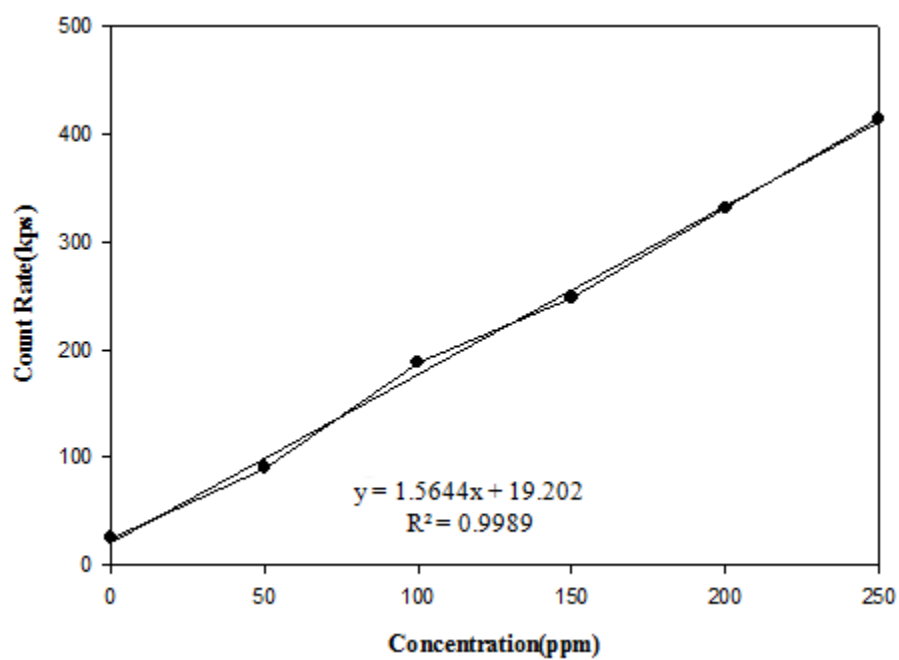
Fig A.1.4 Calibration curve for PEGlyated-SiO_2 is linear
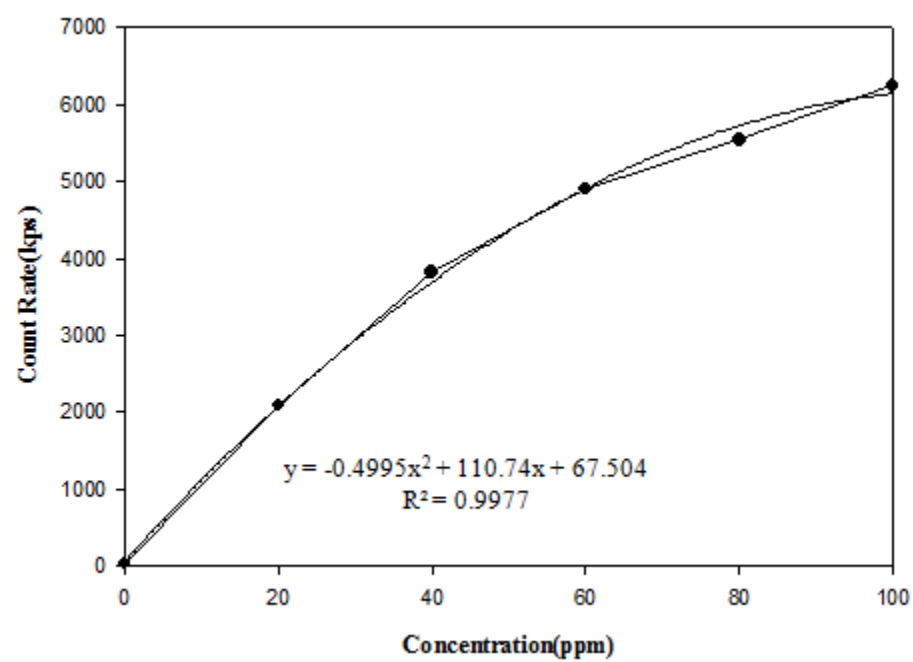
Fig A.1.5 Calibration curve for Y_2O_3

A.2 Dye Adsorption
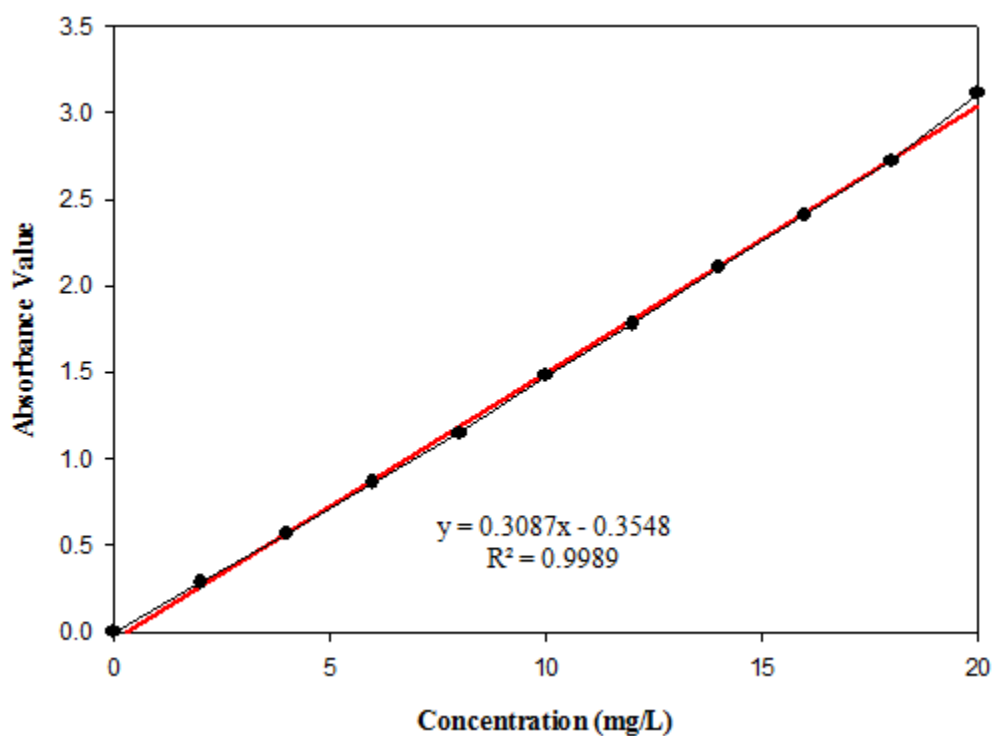
Fig A.2.1 Calibration curve of Rose Bengal

Calibration curve for Rose Bengal dye is linear. Dye concentration was prepared from 0 to 20 mg/L. Each concentration has its own specific absorbance value, and can be used to know the amount of nanoparticles onto the dye.

Dye Concentration (mg/L)	2	4	6	8	10
Absorbance Value	0.2856	0.565	0.863	1.148	1.482
	12	14	16	18	20
	1.778	2.107	2.409	2.723	3.112

Table A.1 Absorbance value of Rose Bengal under specific dye concentration (mg/L)
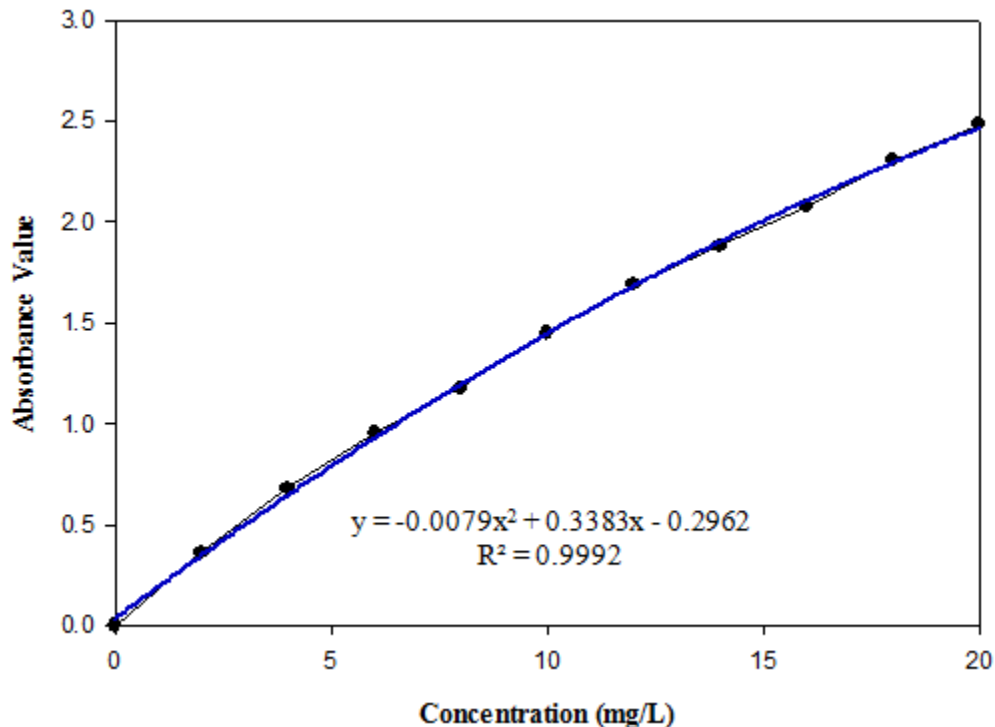
Fig A.2.2 Calibration curve of Nile Blue

Calibration curve for Nile Blue dye is 2nd order. Dye concentration was prepared from 0 to 20 mg/L. Each concentration has its own specific absorbance value, and can be used to know the amount of nanoparticles onto the dye.

Dye Concentration (mg/L)	2	4	6	8	10
Absorbance Value	0.363	0.68	0.951	1.178	1.447
	12	14	16	18	20
	1.691	1.882	2.075	2.304	2.482

Table A.2 Absorbance value under specific dye concentration (mg/L)

Appendix B

NP	dp	E_C	E_V	E_{Amz}	χ_{MeO}	ΔH_{sub}	ΔH_{IE}	ΔH_{sf}	ΔH_{Lat}	$\Delta H_{IE,1+}$	Z^2/r	IEP	ZP
	nm							eV			pm^{-2}	pH	mV
ZnO	22.6 ± 5.1	-3.891	-7.198	7.546	5.674	1.351	28.710	-3.608	42.928	9.394	0.0667	9.6	28.8
CuO	12.8 ± 3.4	-5.174	-6.515	7.719	5.874	3.497	31.515	-1.609	42.856	7.726	0.0548	7.9	7.6
Mn_2O_3	51.5 ± 7.3	-4.647	-7.635	11.709	5.919	2.936	59.677	-9.917	156.975	7.434	0.1552	3.7	-46.1
CoO	71.8 ± 16.2	-4.424	-6.832	9.454	5.735	4.422	29.387	-2.476	39.767	7.881	0.0615	9.2	21.6
Co_3O_4	10.0 ± 2.4	-4.593	-7.025	10.755	5.927	4.422	46.137	-9.380	99.573	7.881	0.1329	9.4	24.6
Cr_2O_3	193.0 ± 90.0	-4.439	-7.524	13.920	5.858	4.120	58.331	-11.717	158.322	6.767	0.1452	5.3	-32.6
Ni_2O_3	140.6 ± 52.5	-4.309	-7.688	11.709	6.052	4.458	65.455	-5.073	164.157	7.639	0.1607	8.3	32.2
Gd_2O_3	43.8 ± 15.8	-2.825	-8.102	16.782	5.499	4.120	42.989	-18.820	134.692	6.150	0.0957	8.0	6.5
In_2O_3	59.6 ± 19	-3.632	-7.322	11.188	5.583	2.518	55.204	-9.606	144.351	5.786	0.1125	9.2	61.9
CeO_2	18.3 ± 6.8	-3.803	-7.450	20.121	5.650	4.354	77.697	-11.284	99.775	5.539	0.1649	7.8	21.4
SiO_2	13.5 ± 4.2	-2.018	-11.118	18.734	6.190	4.664	107.795	-9.410	136.029	8.151	0.6154	1.0	-31.8
Al_2O_3	14.7 ± 5.2	-1.515	-9.815	15.872	5.665	3.429	56.691	-17.345	164.955	5.985	0.1667	7.4	0.0
Y_2O_3	32.7 ± 8.1	-2.352	-8.201	17.433	5.406	4.402	43.362	-19.748	131.676	6.217	0.1000	9.6	42.7
SnO_2	62.4 ± 13.2	-4.013	-8.013	14.397	5.812	3.122	96.334	-5.986	122.369	7.344	0.2319	4.0	-38.8
TiO_2	12.6 ± 4.3	-4.161	-7.491	19.775	5.767	4.902	96.063	-9.779	125.924	6.828	0.2623	6.4	-19.4
ZrO_2	40.1 ± 12.6	-3.192	-8.233	22.723	5.618	6.322	83.379	-11.252	115.954	6.634	0.1905	5.8	-12.8
Fe_2O_3	12.3 ± 2.9	-4.993	-6.987	12.489	5.978	4.306	59.047	-8.512	148.300	7.903	0.1636	7.2	-2.1
Sb_2O_3	11.8 ± 3.3	-3.645	-8.138	10.408	5.514	2.740	53.278	-7.346	142.071	8.608	0.1184	1.0	-35.3
HfO_2	28.4 ± 7.3	-2.956	-8.371	23.938	5.705	6.409	84.863	-1.170	104.812	6.825	0.1928	8.1	33.5
WO_3	16.6 ± 4.3	-5.532	-8.586	24.978	6.640	8.820	213.421	-8.734	250.324	7.864	0.6000	0.3	-61.3
Yb_2O_3	61.7 ± 11.3	-2.831	-7.933	15.091	5.429	1.613	45.092	-18.807	138.672	6.254	0.0909	8.2	9.9
La_2O_3	24.6 ± 5.3	-2.380	-8.147	17.433	5.378	4.467	40.280	-18.668	129.054	5.577	0.0776	9.4	54.3
NiO	13.1 ± 5.9	-3.570	-7.445	9.454	5.744	4.458	30.266	-2.494	40.503	7.639	0.0580	11.4	27.6

[a]d_p: primary nanoparticle (NP) size (given in the format of average size (d) $\pm$ standard deviation (σ)), E_C: NP energy of conduction band, E_V: NP energy of valence band, E_{Amz}: metal oxide atomization energy, χ_{MeO}: metal oxide electronegativity, ΔH_{sub}: metal oxide sublimation enthalpy, ΔH_{IE}: metal oxide ionization energy, ΔH_{sf}: metal oxide standard molar enthalpy of formation, ΔH_{Lat}: metal oxide lattice enthalpy, $\Delta H_{IE,1+}$: first molar ionization energy of metal, Z^2/r: ionic index of metal cation; IEP: NP isoelectric point, ZP: NP zeta potential in water at PH of 7.4; E_{Amz} was converted from the atomization energy in kcal/eqv. The atomization energy of Ni_2O_3 is lacking and thus was estimated as that of Mn_2O_3 since they share the same molecular structure and the atomization energies of NiO and MnO are identical. Note that the enthalpies involved in Born-Haber cycle for Co_3O_4 were calculated by taking the average of those for CoO and Co_2O_3. Also, the Ionic index of the metal ion in Co_3O_4 was estimated as the weighted average (1:2) of Co^{2+} and Co^{3+} in the metal oxide NP crystal.

'Thirty descriptors were used for nano-SAR development. Fourteen of the descriptor values are provided in the Table, while the remaining 16 can be easily calculated as described below.

i. Seven descriptors based on primary NP size were evaluated for SAR development, including: different orders of average size (d^{-2}, d^{-1}, d, d^2), standard deviation (σ), mean/standard deviation ratio (d/σ), and coefficient of variation (σ/d);

ii. Three other quantum mechanics descriptors were derived from E_C and E_V, including chemical potential ($\mu=(E_C+E_V)/2$), chemical hardness ($\eta=(E_C-E_V)/2$), and electrophilicity ($\omega=\mu^2/2\eta$);

iii. Fundamental metal oxide descriptors were also included in the initial pool of descriptor, including numbers of metal and oxygen atoms, atomic mass of metal and metal oxide molecular weight, group and period of metal (in periodic table), and electronegativity of metal; these are not listed in the above table as they can be easily ascertained from the metal oxide chemical formula.

Fig B.1 Physicochemical properties of nanoparticles (Liu, Zhang et al. 2013).